Bioconjugate Chemistry

Article

Design, synthesis, and use of MMP-2 inhibitor-conjugated quantum dots in functional biochemical assays.

Erika Bourguet, Kristina Brazhnik, Alyona Sukhanova, Gautier Moroy, Sylvie Brassart-Pasco, Anne-Pascaline Martin, Isabelle Villena, Georges Bellon, Janos Sapi, and Igor Nabiev

Bioconjugate Chem., **Just Accepted Manuscript** • DOI: 10.1021/acs.bioconjchem.6b00065 • Publication Date (Web): 01 Mar 2016

ACS Publications

Bioconjugate Chemistry is published by the American Chemical Society. 1155 Sixteenth Street N.W., Washington, DC 20036

Design, synthesis, and use of MMP-2 inhibitor-conjugated quantum dots in functional biochemical assays.

Erika Bourguet[*,†], Kristina Brazhnik[‡,§], Alyona Sukhanova[‡,§], Gautier Moroy[‖], Sylvie Brassart-Pasco[⊥], Anne-Pascaline Martin[⊥,#], Isabelle Villena[#], Georges Bellon[⊥], Janos Sapi[†], Igor Nabiev[‡,§]

[†] Institut de Chimie Moléculaire de Reims, UMR 7312-CNRS, SFR Cap-Santé, UFR de Pharmacie, Université de Reims Champagne-Ardenne, 51 rue Cognacq Jay, 51100 Reims, France

[‡] Laboratoire de Recherche en Nanosciences, LRN - EA4682, UFR de Pharmacie, Université de Reims Champagne-Ardenne, 51 rue Cognacq Jay, 51100 Reims, France

[§] Laboratory of Nano-Bioengineering, National Research Nuclear University MEPhI (Moscow Engineering Physics Institute), 31 Kashirskoe shosse, 115409 Moscow, Russian Federation

[‖] Molécules Thérapeutiques *In Silico*, INSERM UMR-S 973, Université Paris Diderot, Sorbonne Paris Cité, 35 rue Hélène Brion, 75013 Paris, France

[⊥] Laboratoire de Biochimie et de Biologie moléculaire, MEDyC, UMR CNRS/URCA 7369, SFR Cap-Santé, UFR de Médecine, Université de Reims Champagne-Ardenne, 51 rue Cognacq Jay, 51100 Reims, France.

[#] Laboratoire de Parasitologie-Mycologie, EA3800, SFR Cap-Santé, UFR de Médecine, Université de Reims Champagne-Ardenne, 51 rue Cognacq-Jay, 51100 Reims, France.

ABSTRACT: The development of chemically designed matrix metalloprotease (MMP) inhibitors has advanced the understanding of the roles of MMPs in different diseases. Most MMP probes designed are fluorogenic substrates, often suffering from photo- and chemical instability and providing fluorescence signal of moderate intensity, which is difficult to detect and analyze when dealing with crude biological samples.

Here, an MMP inhibitor that selectively inhibits MMP-2 more strongly than Galardin® has been synthesized and used for enzyme labelling and detection of the MMP-2 activity. A complete MMP-2 recognition complex consisting of a biotinylated MMP inhibitor tagged with the streptavidin-quantum dot (QD) conjugate have been prepared. This recognition complex, which is characterized by a narrow fluorescence emission spectrum, long fluorescence lifetime, and negligible photobleaching, has been demonstrated to specifically detect MMP-2 in *in vitro* sandwich-type biochemical assays with sensitivities orders of magnitude higher than those of the existing "gold standards" employing organic dyes.

The approach developed can be used for specific *in vitro* visualization and testing of MMP-2 in cells and tissues with sensitivities significantly exceeding those of the best existing fluorogenic techniques.

KEYWORDS: *matrix metalloproteinases, matrix metalloproteinase inhibitors, selective MMP-2 inhibition, molecular modelling, quantum dots.*

INTRODUCTION

Studying biological processes at the molecular level within a living cell is a major challenge for cell biology investigation.[1,2] Similarly, spatiotemporal tracking of small molecules in *ex vivo* or *in vivo* environment gives a better insight into their interactions with proteins, rendering target identification more efficacious and, *in fine,* accelerating drug development. The existing techniques based on spectroscopic and biooptical methods using organic dyes are mostly limited by the difficulties in imaging individual molecules in the optically noisy cellular environment and accessing directly the interior of living cells.[3] As promising alternative tools, semi-conductor nanocrystals quantum dots (QDs) have emerged for numerous biomedical applications,[4,5] such as cellular labeling, biochemical sensing, probing biocatalyzed reactions, and drug delivery.[6]

QDs are characterized by their narrow, composition and size dependent, emission wavelength[7], extreme brightness, rock-solid photostability and chemical robustness.[8] QD fluorescence covers the optical spectrum from the near-UV to the IR, which provides a unique possibility for multiplexing, unlike with the use of organic dyes.[9] Even if QDs possess optical properties for biological applications, nanoparticles need to be functionalized to achieve a convenient solubility in aqueous media and *in fine* hydrophilic ligands may be used as anchor points for biomolecules such as peptides, DNA or drugs.[10] The hydrophobic outer shell of QDs may be exchanged or chemically reacted with bi- or multifunctional molecules containing capping ligands, cationic polymers or liposomes bearing cell penetrating peptide (CPP)[11,12], or with amphiphilic polymers.[13,14] Biomolecules may be attached to their surface by covalent binding *via* different surface functional groups (amino, thiol, carboxyl…), or through non-covalent streptavidin/biotin, electrostatic or ionic interactions.[15,16]

Matrix metalloproteinases (MMPs) belong to the family of zinc-dependent proteases involved in the degradation and remodelling of extracellular matrix proteins. The activity of MMPs is controlled by endogenous tissue inhibitors of metalloproteinases (TIMPs). The finely tuned MMPs/TIMPs balance found in normal physiological processes (tissue modeling, angiogenesis,

wound healing, embryonic growth…) is disrupted in several pathologies such as atherosclerosis, aneurysm, pulmonary emphysema and cancer... Among more than 25 MMPs, MMP-2 (gelatinase A) plays an important role in tumorigenesis, particularly in cancer progression[17] rendering this enzyme a therapeutic and diagnostic target[18] for drug development and *in vivo* detection of tumour growth or invasion. Thus, the conception of potent and MMP-2 selective inhibitors may constitute a valuable therapeutic approach for melanoma.[19]

In the past two decades, several pseudo-dipeptide-type inhibitors, such as batimastat, marimastat, and ilomastat (Galardin®) were synthesized with the aim to regulate imbalanced proteolytic activity (Figure 1). Although, first generation of MMP inhibitors, in spite of their high potency and preliminary clinical trials, have been withdrawn before advanced clinical experiments due to severe musculoskeletal side effects. They may be considered as starting points for the design and development of selective MMP inhibitors with better physicochemical and pharmacological profiles. These efforts took two directions: (1) exploration of structural differences in the substrate-binding regions around the zinc cation and (2) design of new zinc-binding groups (ZBG).

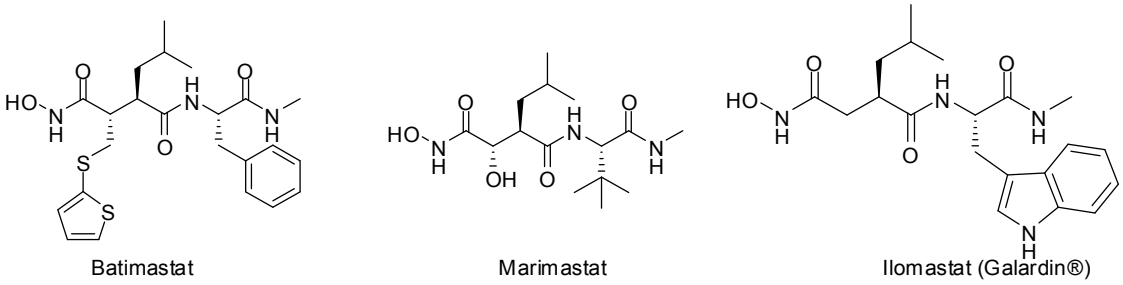

Figure 1. The structure of highly efficient inhibitors: batimastat, marimastat, and ilomastat.

Although matrix metalloproteinases have a great homology of sequence, the size, shape, depth, and conformational mobility of side pockets (denoted S1, S2, S3 for the non-primed side and S'1, S'2, S'3 for the primed side around the zinc-containing catalytic site), are determinant for inhibitory potency and selectivity.[20,21] Studies on structure-activity relationship have shown that the subsite selectivity decreases in the following order: S'1 > S2, S'3, S3 > S1 > S'2.[22,23]

Thus, attempts at obtaining selectivity among MMP enzymes have concentrated on the S'1 subsite, called the specificity pocket.[24,25] The S'1 pocket of MMP-2 is hydrophobic, forms a large, nearly bottomless channel, and the S'1 loop is flexible to accommodate more bulky ligands.[26] Thus, modifications of P'1 group in MMP inhibitors (MMPIs) ensure selectivity among MMP-family members. Since the succinyl hydroxamate backbone is a common feature in the most efficient first-generation MMP binders[27], pharmacomodulation was carried out at this structural unit.

For this purpose, Miller *et al*.[28] observed the maximum specificity of the inhibitor for MMP-2 in comparison to MMP-1 with addition of a C12 alkyl chain as the P'1 group into the structure of batimastat (IC_{50} = 1 and 50000 nM, respectively). Broadhurst *et al.*[29] have described a marimastat analog containing a C9 linear chain displaying a good MMP-2 inhibitory activity (IC_{50} < 0.15 nM).[30] However, Miller *et al*.[28] described the best selectivity for MMP-2 *versus* MMP-1 with a compound containing a C16 alkyl chain (IC_{50} = 0.6 and 5000 nM, respectively). Levy *et al*.[31] modified ilomastat by elongating its alkyl chain to eight carbon atoms. Neither inhibitory activity nor selectivity were ameliorated.

MMP inhibitors contain hydroxamic acid as a zinc-binding group (ZBG). Although this function has proved to be a very strong ZBG, toxicity, low bioavailability, and *in vivo* unstability of this chemical entity associated with severe side effects have resulted in the development of alternative ZBG such as carboxylic acid, a precursor of the hydroxamate group.

Batimastat and marimastat analogs bearing a C16 alkyl chain in P'1 position with carboxylic acid type ZBG showed a lowest MMP-2 inhibitory activity (IC_{50} = 50 and 30 nM, respectively).

Reliable techniques are crucial for hit detection, biological evaluation of compound collections, or monitoring enzyme inhibitory activities. By the past, conventional techniques included gel electrophoresis[32], fluorescence (near-infrared)[33-40], or magnetic-resonance-based approaches[41-43] were used to detect MMPs activity, but recently much attention has been paid to Förster resonance energy transfert (FRET) for assay of proteases.[44-46]

QD-FRET-based protease sensors exploiting QDs as donor and rhodamine or gold nanoparticle as acceptor have also been developed to survey collagenase activity[47-49] in normal and cancer cells.[50] QDs can also act as energy acceptors in bioluminescence resonance energy transfer (BRET) from a protein energy donor, such as a mutant form of *Renilla* luciferase, to detect protease activity.[51,52] QD-based methods have also been used for multiplexed detection and imaging of several MMPs (MMP-2 and MMP-7)[52,53] and multiplexed protease inhibition and competition (folic acid and MMP-7) assays.[48,54] In these methods, the MMP activity is identified by changes in QD fluorescence resulting from the cleavage of a specific enzyme-recognizing peptide attached to the QDs. Other approaches employ QDs coupled to antibodies or MMP-9-siRNA to study the enzymatic activity of MMP-9[55] or the MMP-9 gene expression in the brain.[56]

Herein, we describe the synthesis and preliminary biological evaluation of a range of ilomastat derivatives bearing carboxylic acid as a ZBG and alkylidene chains of different lengths at the P'1 position. Additional pharmacomodulations were made at the C-2 position of the indole ring to evaluate the impact of a bulky phenyl substitution, P'2 group, on MMP inhibition activity. Among these derivatives, the most selective MMP-2 inhibitor (**4k**) was conjugated to QDs to use it as probe to identify MMP-2 enzyme activity. The advanced optical properties of streptavidin-QD conjugates, the high binding constant for streptavidin-biotin interaction and the technical simplicity of mixing streptavidin-QD nanoparticles with the biotinylated ligand (**4k**) make this approach an attractive tool to generate imaging probes with potential *in vitro* applications in advanced biochemical MMP-2 assays (Scheme 1).

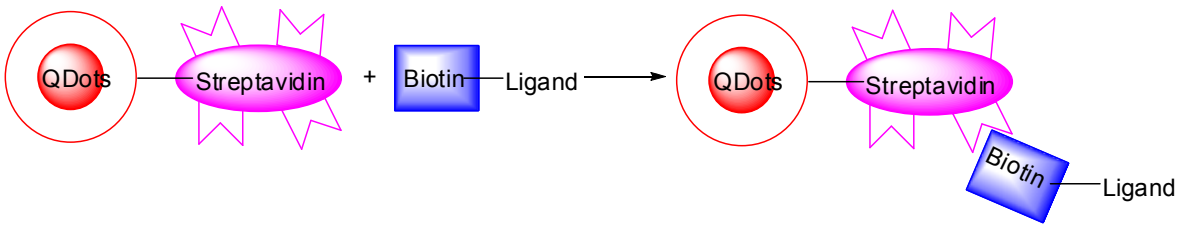

Scheme 1. Non-covalent coupling of a biotinylated compound and a fluorescent QD-streptavidin conjugate.

RESULTS AND DISCUSSION

Influence of the P'1 part of ilomastat on gelatinase inhibition

For a decade, we have been involved in the pharmacomodulation of ilomastat, focusing recently our efforts on designing analog derivatives with a modified P'1 succinic component.

First, incorporation of one unsaturation at the P'1 position aiming at increasing the hydrophobicity and conformational rigidity was considered. Replacement of the isobutyl group of ilomastat with an isobutylidene function **1** with the *E* geometry improved the selectivity for MMP-2 *versus* MMP-3 (IC_{50} = 1.3 and 179 nM, respectively) (Figure 2).[57] Pursuing these pharmacomodulations, we synthesized other dehydro and didehydro analogs (**2a-d**).[58]

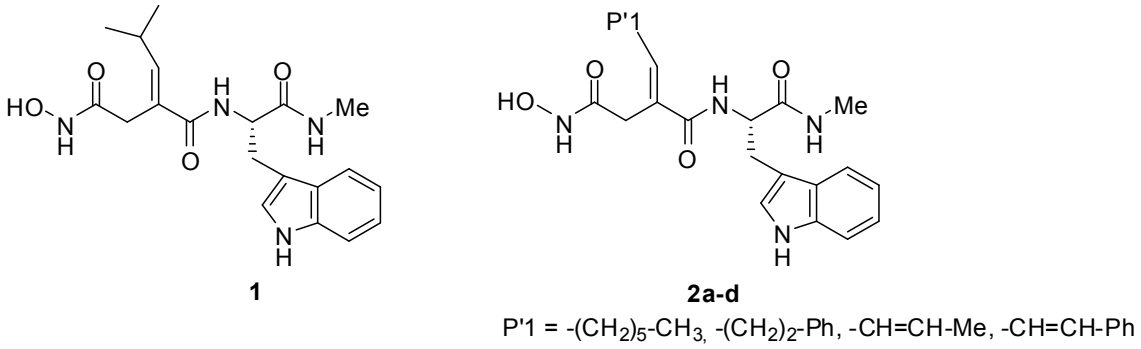

Figure 2. Pharmacomodulation of the P'1 group.

The inhibitory activities of these analogs for all MMPs were decreased as compared to ilomastat (Galardin®). However, analog **2a** with a C7 alkyl chain displayed an interesting selectivity for MMP-2 compared to MMP-9 (IC_{50} = 123 and > 10^4 nM, respectively) indicating that the S'1 pocket of MMP-2 is sufficiently deep to accommodate long alkyl chains.

Influence of the P'2 part of ilomastat on gelatinase inhibition

Introduction of an amino-alkyl chain at the C2 position of the indole ring leads to a decrease in the MMP inhibitory activity but greatly improves the selectivity for MMP-2.[57] In this line, a phenyl group was introduced at the C2 position through the Suzuki reaction[59,60] (Figure 3) and the obtained analog **3** was shown to have enhanced potency and selectivity for MMP-2 *versus* MMP-1 (IC_{50} = 0.092 and 0.244 nM, respectively).[61]

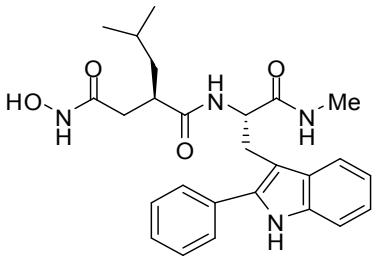

3

Figure 3. Pharmacomodulation of the P'2 group.

In order to clarify the mode of interaction between MMP-2 and analog **3**, molecular docking computations have been carried out using the AutoDock software.[62,63] As expected, the hydroxamate group chelates the Zn atom in the lowest-energy binding mode (Figure 4a). Moreover, the carbonyl function of the hydroxamate group is involved in H-bond interaction with Ala_{192}. The isobutyl group is located in the S'1 subsite forming van der Waals interactions with Leu_{191}, Ala_{192}, Val_{400}, His_{403}, Pro_{423}, and Tyr_{425}. The modified indole ring is located in the S'2 subsite and is oriented towards the solvent. In addition, four H-bonds between compound **3** and MMP-2 amino acid residues located in the S'3 subsite, namely, Gly_{189}, Leu_{191}, Pro_{423}, and Tyr_{425}, (highlighted) stabilize this model (Figure 4b).

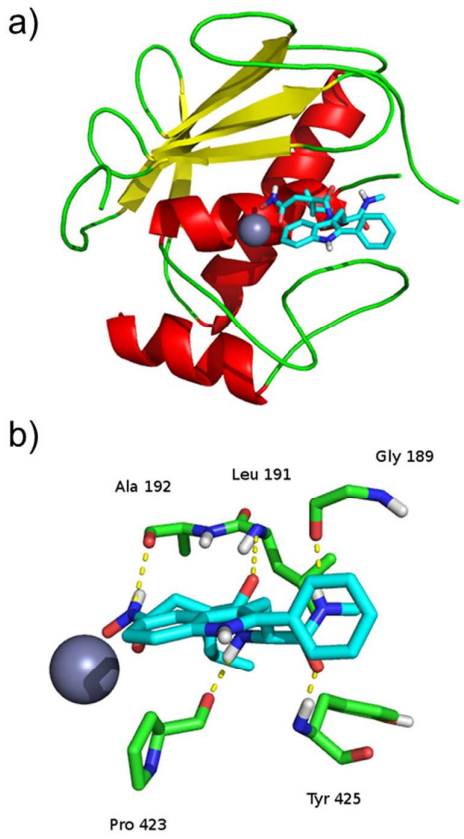

Figure 4. Docking of analogue **3** in the structure of MMP-2.

a) The binding mode of analogue **3** with MMP-2;

b) A detailed view of the H-bonds enabling the model stabilization.

It is well-known that the large and solvent-exposed S'2 pocket is flexible to accommodate bulky and hydrophobic groups[30,64] and aromatic groups are in agreement with this model as supported by *in vitro* activity.[65]

Influence of the P'1 and P'2 parts of ilomastat on gelatinase inhibition

In order to further improve the selectivity for MMP-2, the alkyl chain was elongated by 8 to 20 carbon atoms using a method described previously[58] and a phenyl group was also introduced at the C2 position of the indole part through the Suzuki reaction (Figure 5).[66] Replacement of the very strong hydroxamic acid Zn-chelating group by a less complexing carboxylate function may also favour selectivity to the detriment of affinity. For comparison, ilomastat and compound **3b**

were also included in the series of biological evaluations (Table 1).[31,67] As shown in Table 1, the carboxylate counterpart **3b** is more selective for MMP-1 (among other MMPs) than ilomastat, although its inhibitory activity is decreased.

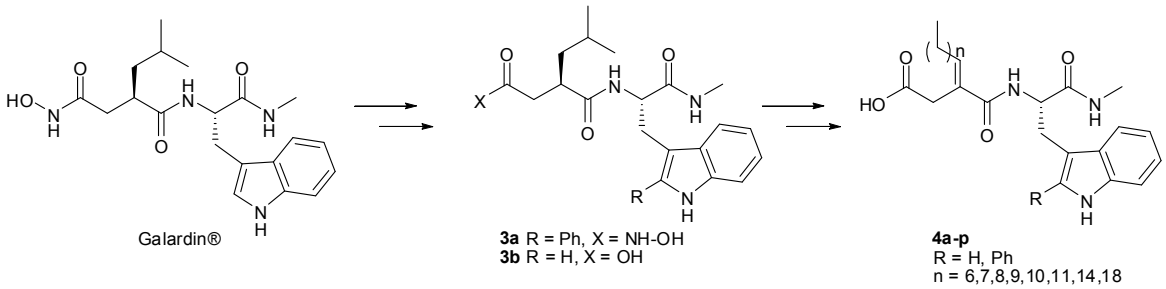

Figure 5. Pharmacomodulation of the ZBG, the P'1 and P'2 groups.

In an agreement with the literature data, the inhibitory activity values for compounds **4a-p** are detrimental for affinity compared to ilomastat (Galardin®) but remain of the same order of magnitude as that found for the carboxylic-acid-type ilomastat analogue **3b**.

Contrary to our expectations, elongation of the alkyl chain with an incorporated unsaturation did not improve the inhibitory activity of the compounds towards MMP-2. However, we found an increased selectivity of the C10 analog **4c** (n = 8, R = H) for MMP-9 *versus* MMP-1.

Furthermore, the ilomastat derivative **4k** (n = 8, R = Ph) with a C10 alkyl chain and a phenyl group at the P'2 position displayed the best selectivity for MMP-2 inhibition (IC_{50} = 80 nM) in comparison to other MMPs (Table 1), demonstrating that a carboxylate type ZBG may be an alternative for a finely tuned balance between enzyme activity and selectivity. In addition, this pharmacomodulation helps to avoid the toxicity and side effects known about the parent ilomastat-type molecules.

Table 1. P'1- and P'2-modified ilomastat inhibitors. The IC_{50} values are expressed in nM.

Compounds	n	R	MMP-1	MMP-2	MMP-9	MMP-13	MMP-14
Ilomastat	-	H	1.5	1.1	0.5	-	13.4
3b	-	H	9.9[a]	170[b]	100[b]		1260[a]
4a	6	H	> 10^5	7570	838	992	> 10^5
4b	7	H	> 10^5	458	241	1280	> 10^5
4c	8	H	> 10^5	247	173	925	> 10^5
4d	9	H	> 10^5	249	450	243	> 10^5
4e	10	H	> 10^5	351	211	244	> 10^5
4f	11	H	> 10^5	655	673	515	> 10^5
4g	14	H	> 10^5	762	582	155	> 10^5
4h	18	H	> 10^5	> 10^5	> 10^5	1277	> 10^5
4i	6	Ph	> 10^5	670	297	1573	> 10^5
4j	7	Ph	5182	976	339	1062	> 10^5
4k	8	Ph	1190	80	320	1068	> 10^5
4l	9	Ph	3085	501	554	459	> 10^5
4m	10	Ph	4151	459	581	555	> 10^5
4n	11	Ph	> 10^5	568	768	607	> 10^5
4o	14	Ph	> 10^5	1235	982	185	> 10^5
4p	18	Ph	> 10^5	> 10^5	1395	245	> 10^5

[a] Unpublished results[68]

[b] Ki values are expressed in nM

According to the docking computations, the lowest-energy binding modes are characterized by chelation of the Zn atom with the carboxylate group of **4k** in the MMP-2 active site. Four H-bonds are formed between the pseudopeptide backbone of the **4k** analog and MMP-2 residues, located at the upper (Gly_{189} and Leu_{191}) and lower (Pro_{423} and Tyr_{425}) rims of the S'3 subsite. The modified P'2 group in the S'2 subsite is exposed to the solvent. The long alkyl chain is inserted into the S'1 pocket, inducing van der Waals interactions with Leu_{399}, Val_{400}, His_{403}, Ala_{419}, Leu_{420}, Ala_{422}, Pro_{423}, Ile_{424}, Tyr_{425}, Thr_{426}, Thr_{428}, and Phe_{431} (Figure 6).

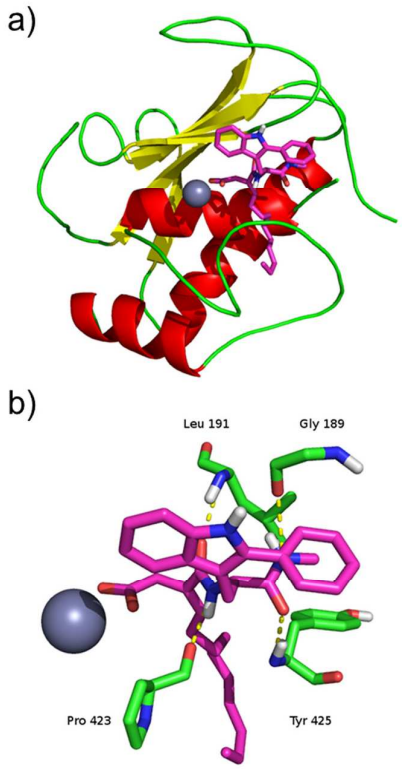

Figure 6. Docking of analogue **4k** in the structure of MMP-2.

(a) The binding mode of analogue **4k** with MMP-2;

(b) A detailed view of the H-bonds enabling the model stabilization.

We have also investigated the binding mode of compound **4k** with MMP-9. In the lowest-energy docked conformation predicted by AutoDock, the Zn atom is chelated by the carboxyl group and four H-bonds are formed with Gly_{186}, Leu_{188}, Pro_{421}, and Tyr_{423} located in the S'3 subsite. The modified P'2 group in the S'2 subsite is exposed again to the solvent. The long alkyl

group is stabilized in the S'1 subsite by several van der Waals interactions formed by the following amino acids: Leu_{397}, Val_{398}, His_{401}, Ala_{417}, Leu_{418}, Tyr_{420}, Met_{422}, Tyr_{423}, Arg_{424}, and Thr_{426} (Figure 7).

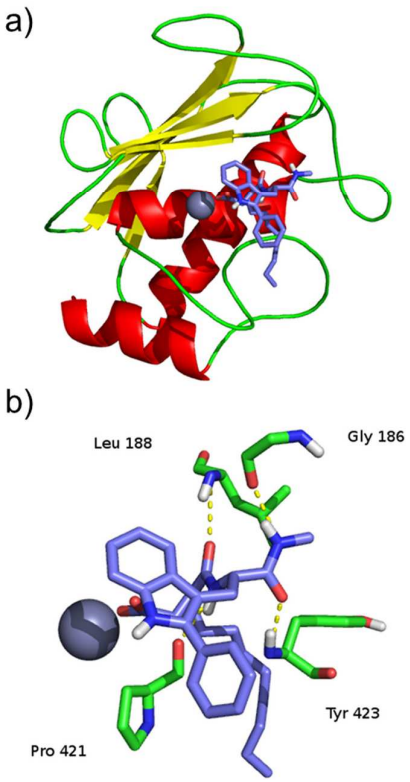

Figure 7. Docking of analogue **4k** in the structure of MMP-9.

(a) The binding mode of analogue **4k** with MMP-9;

(b) A detailed view of the H-bonds enabling the model stabilization.

As a result of preliminary modelling and examination studies, the most appropriate compound, **4k**, was selected for further evaluation and estimation of its inhibitory activity and effects on cell migration and invasion. MMP-2 proteolytic activity was measured in the presence or absence of the inhibitor using a fluorescent Dye Quenched substrate (DQ) gelatin.

Concanavalin A treatment of cells induces active MMP-14 expression on the cell surface, ensuring rapid MMP-2 activation and release into the culture medium.[69] In the presence of compound **4k**, the MMP-2 activity was reduced by 20%, while ilomastat (Galardin®) decreased the enzyme activity by 30% (Figure 8).

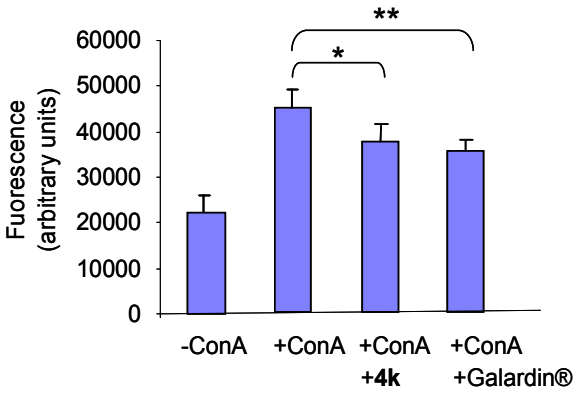

Figure 8. MMP-2 proteolytic activity measurement.

HT-1080 cells were treated overnight with concanavalin A. Cells were then pre-incubated with or without the effector (100 µM **4k** or 10 µM Galardin®) for 1 h and then with Dye Quenched substrate (DQ gelatin) (500 ng/300 µL per well). Fluorescence was measured at 525 nm. *: $p<0.05$; **: $p<0.01$.

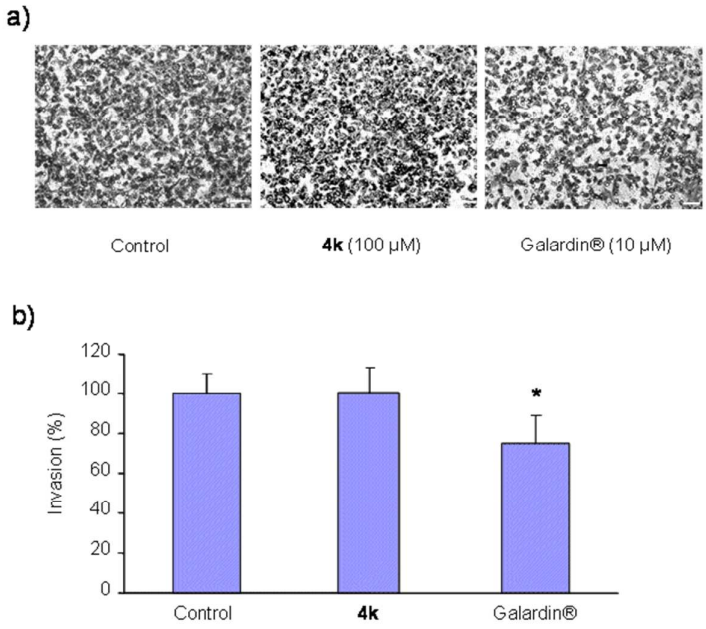

Figure 9. HT-1080 cell invasion rate estimated by the ability of cells to migrate through Matrigel®-coated membranes upon treatment with compound **4k** or ilomastat (Galardin®).

a) A representative photomicrograph showing cell invasion after 6 h of incubation.

b) A representative bar graph quantifying cell invasion. *: $p<0.1$. Scale bar, 50 µm.

HT-1080 cell invasion was also estimated *in vitro* in the presence of compound **4k** or ilomastat. HT-1080 cells were tested for their ability to migrate through Matrigel®-coated (20 µg/well) filters during 6 h. Compound **4k** did not alter cell invasion (Figure 9), while ilomastat inhibited cell migration by 25%.

During the invasion process, HT-1080 cells produce different types of MMPs (MMP-14, MMP-2, *etc*.) and serine proteinases (u-PA, t-PA, *etc*.) which are involved in cell migration. Evidently, compound **4k** mainly blocks the MMP-2 activity and is a selective MMP-2 inhibitor, but its involvement in the migration process is probably insignificant, which explains the absence of inhibitory effect on HT-1080 cell invasion. Ilomastat (Galardin®) inhibits different types of MMPs, including MMP-14, which is known to degrade extracellular matrix, to activate proMMP-2 and to greatly favour tumor cell invasion. This could explain the observed inhibitory effect on HT-1080 cell invasion (25%).

Synthesis of a biotinylated inhibitor 4k

In line with our goal providing tools for imaging, we investigated the feasibility of MMP inhibitor-QDs conjugates. The selected compound **4k** was modified at the indole NH group in order to insert the biotin compound into the inhibitor structure (Figure 10). Biotin interacts non-covalently with streptavidin with an extremely high affinity ($K_D \simeq 10^{15}$ M^{-1}), resulting in the formation of a highly-stable specific biotin-streptavidin complex, which is widely employed in numerous biological approaches.[70,71]

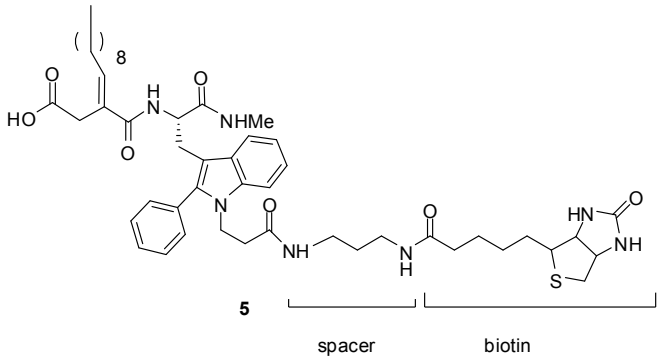

Figure 10. Structure of the resultant biotinylated compound **4k**.

Modification of compound **4k** with biotin included several steps. First, the tryptophan derivative **8** obtained from derivative **7** using the Suzuki reaction[72] was treated with *t*-butylacrylate (Michael reaction) to obtain compound **9** with a yield of 90%. The obtained functionalized indole derivative **9** was subjected to transamidification and deprotected with a yield of 80% and coupled to compound **11** to obtain compound **12** with a yield of 82% (Scheme 2).

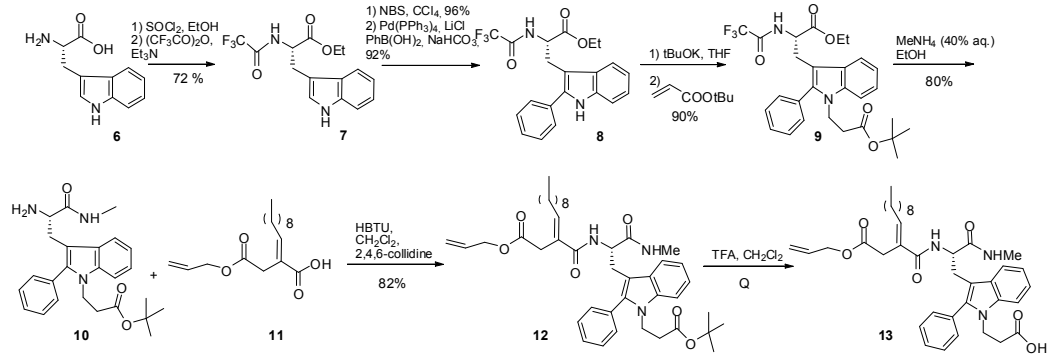

Scheme 2. Preparation of the substituted analogue **13**.

The biotinylated diaminoalkyl spacer **16** was obtained by coupling mono-protected diaminopropan **14** and biotin **15** with a yield of 74% (Scheme 3).

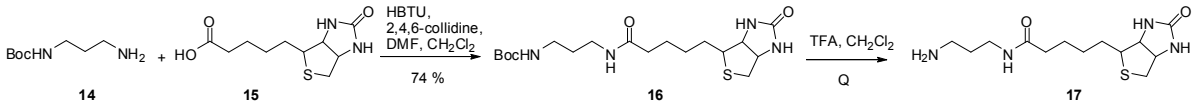

Scheme 3. Preparation of the biotinylated linker **17**.

In the next step of the synthesis, the deprotected pseudo-dipeptide **13** was reacted with the deprotected biotinylated diaminoalkyl spacer **17** to obtain compound **18** with a yield of 38% in two consecutive steps. From compound **18**, the allyl-protecting group was removed upon treatment with the catalyst $Pd(Ph_3P)_4$ to obtain compound **5** with a yield of 72% (Scheme 4).

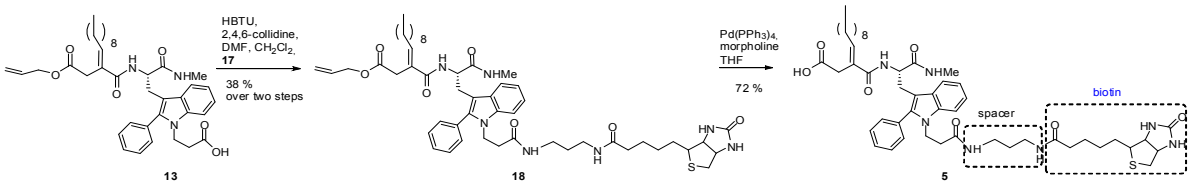

Scheme 4. Synthesis of the compound **5**.

Compound **5** was also submitted to MMP-2 inhibition assay by using a classical gelatin zymography made under the same conditions as described for compound **4k**. Comparative study showed that compound **5** ensured a 34% inhibition of the enzyme *versus* 45% inhibition with compound **4k**, indicating that biotinylation only slightly decreased the inhibitory activity towards MMP-2 (Figure 11). Subsequently, compound **5** served as a basis for our further experiments.

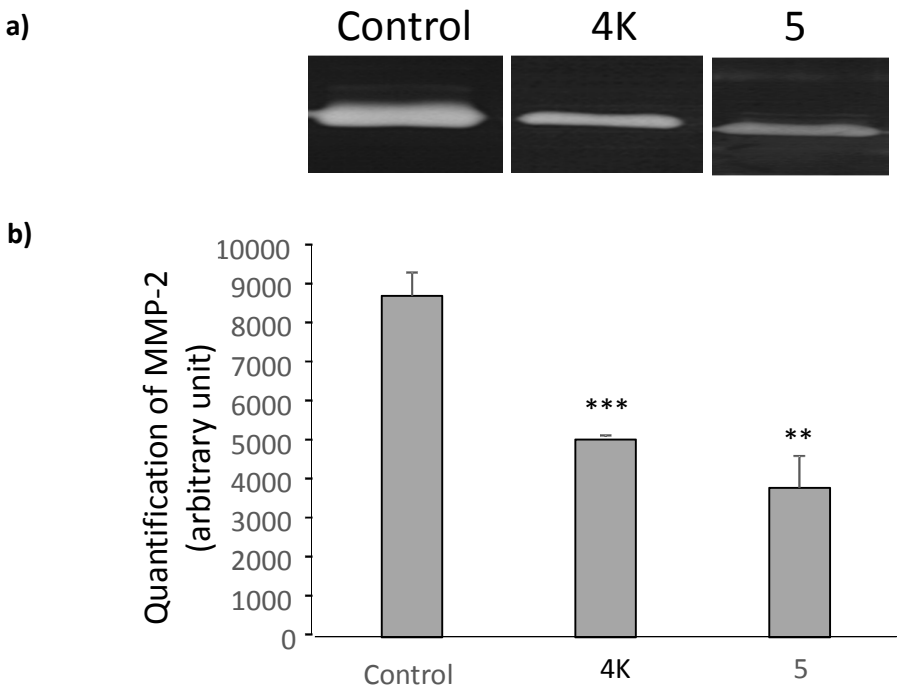

Figure 11. Inhibition of MMP-2 gelatinolytic activity.

a) Results of zymography analysis: 0.4 ng of active MMP-2/well were resolved in gelatin zymography. Each lane was incubated overnight in 50 mM Tris buffer, pH 7.5, with 200 mM NaCl and 5 mM $CaCl_2$ without (control) or with 10 µM inhibitor (compound **4k** or compound **5**); b) Quantification of MMP-2 gelatinolytic activity by densitometry. ***: $p<0.001$; **: $p<0.005$.

MMP-2 inhibition with the designed inhibitor 5

The MMP-2 activity was estimated in standard gelatinase/collagenase assay based on digestion of an internally quenched fluorescent substrate with an activated enzyme. The efficiency of substrate digestion resulting in an increase in dye fluorescence was measured continuously at multiple time points. The fluorescence of the digested product increased proportionally to the enzyme proteolytic activity and the amount of activated MMP-2 (Figure 12a). In the presence of the designed inhibitor **5**, the protease gelatinolytic activity decreased proportionally to an increase in the concentration of inhibitor, resulting in quenching of the fluorescence of the undigested substrate (Figure 12b). We have found that addition of 100 ng of compound **5** to 50 ng of MMP-2 reduces the protease activity by 50%. Increasing the amount of the inhibitor leads to stronger enzyme inactivation.

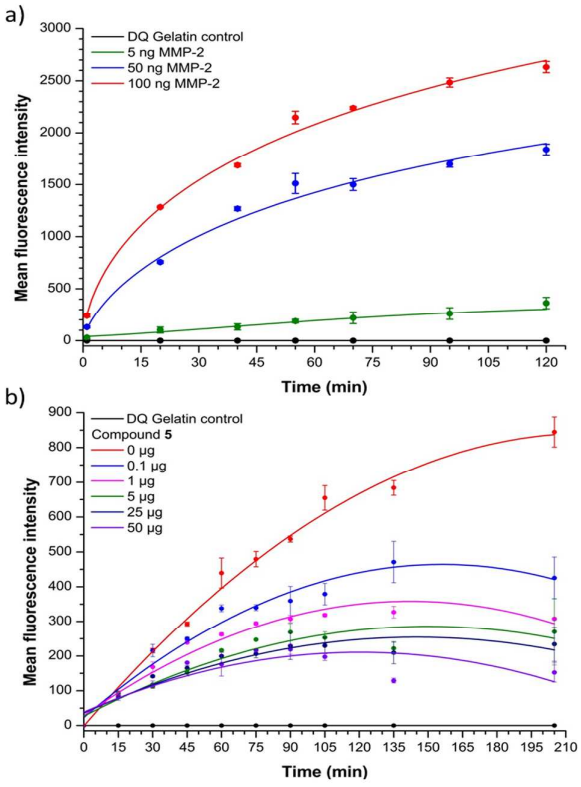

Figure 12. Influence of compound **5** on MMP-2 activity as determined by Dye Quenched substrate (DQ gelatin) digestion.

a) MMP-2 activity at different concentrations of pre-activated enzyme resulting in an increase in fluorescein fluorescence.

b) Concentration-dependent effect of compound **5** on MMP-2 activity. Each analysis has been performed in duplicate ($p<0.001$).

We have further coupled the MMPI biotinylated compound **5** to fluorescent QD-streptavidin conjugate in order to detect the MMP-2 in different *in vitro* assays and to compare QD-based assays with those based on organic dyes.

MMP-2 ultrasensitive detection with QD-tagged compound 5

According to the manufacturer's (Invitrogen) protocol, the number of streptavidin molecules per QD may be estimated as 5 to 10, depending on the QD batch, emission wavelength, and steric effects of the bound streptavidin. Typically, a streptavidin molecule contains four biotin binding sites[71,73] enabling coupling from 20 to 40 biotinylated compounds per QD-streptavidin conjugate. However, it was shown that, due to the steric effects, only one or two binding sites are easily accessible for biotin on the surface of a QD-streptavidin conjugate.[73,74]

Dot-blotting of the biotinylated MMP-2 inhibitor

Formation of an effective complex of compound **5** with streptavidin-QD565 conjugate was visualized using the dot-blot technique. Biotinylated compound **5** diluted in methanol severely damaged and dissolved nitrocellulose membrane and was only detectable in amounts above 2 μg. Depositing these samples on a polyvinylidene difluoride (PVDF) membrane allowed the detection of 1 μg of the inhibitor as the lowest detection limit (data not shown). When dissolved in dimethyl sulfoxide (DMSO) and subsequently diluted in phosphate buffered saline (PBS), the inhibitor can be loaded on a nitrocellulose membrane without any damaging and is detectable in amounts of 0.2 to 1 μg as the lowest detection limit (Figure 13).

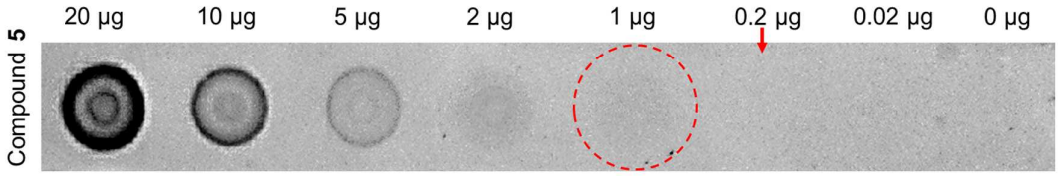

Figure 13. Detection of biotinylated compound **5** with the fluorescent streptavidin-QD 565 nm conjugate using the dot-blot technique.

*In vitro sandwich-type assay for MMP-2 detection using the designed QD-coupled inhibitor **5**.*

The formation of a complete complex consisting of MMP-2 enzyme, biotinylated inhibitor **5**, and fluorescent conjugate of streptavidin with QD800 nm was performed by means of solid-state sandwich-type analytic biochemical assay. Here, 50 ng of MMP-2 was used in MMP-2 activity assays, since this amount of active enzyme was estimated to efficiently and quickly digest the gelatin substrate. The proenzyme was activated with *p*-amino phenylmercuric acetate before adsorption in order to provide appropriate conformation of the inhibitory-binding sites. Activated MMP-2, MMP-2 or the same quantity of BSA protein control were adsorbed on a treated 96-well plate in PBS (pH 7.4). Increasing amounts of biotinylated compound **5** and QD-streptavidin conjugate were subsequently incubated with the adsorbed MMP-2. The QD fluorescence intensity increased proportionally to the biotinylated inhibitor amount in the range from 0 to 100 µg (Figure 14). Thus, the complex of MMP-2 with the designed biotinylated compound **5** can be quantitatively detected and visualized using compact and bright QD-streptavidin conjugates.

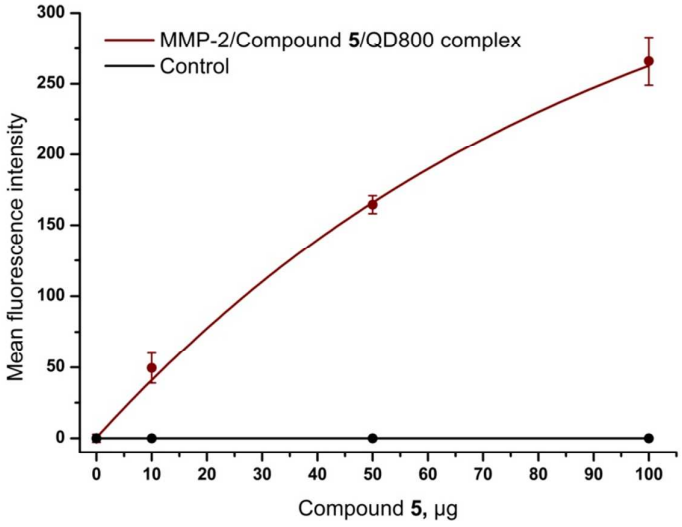

Figure 14. Quantitative detection of MMP-2/biotinylated compound **5** complex with the fluorescent streptavidin-QD800 nm conjugate in *in vitro* sandwich-type biochemical assays. In a control experiment, BSA was used instead of MMP-2. Each analysis has been performed in duplicate ($p<0.001$).

We performed additional experiments in order to explore the photostability of QDs enabling long-term accumulation of their fluorescence signal accompanied by order-of-magnitude improvements of the signal-to-noise ratios in fluorogenic assay and, consequently, increasing the sensitivity for application of QD-based conjugates to MMP-2 detection *in vitro* and to compare the sensitivity of QD-based assays with those based on organic dyes.

Figure 15 shows that accumulation of the signal from the fluorogenic assay employing strepta-QD conjugate for visualization of MMP-2-inhibitor complexes leads to an increase in the signal-to-noise ratio in the given detection scheme by more than two orders of magnitude and, hence, the corresponding increase in the sensitivity of detection of the inhibitor-MMP-2 complex. This increase may reach even higher values if longer signal accumulation times and optimized detection schemes are employed. The result shown in Figure 15 was achieved due to the rock-solid photostability of QDs enabling long-term QD fluorescent signal accumulation

without significant photobleaching of the nanocrystals. Such a photostability is not characteristic of the organic dyes used in currently available fluorogenic assays. Therefore, we have performed additional comparative study of the model biochemical assays employing different organic dyes in parallel with the assays employing strepta-QD conjugates in order to compare the changes in their state during long-term signal detection and accumulation.

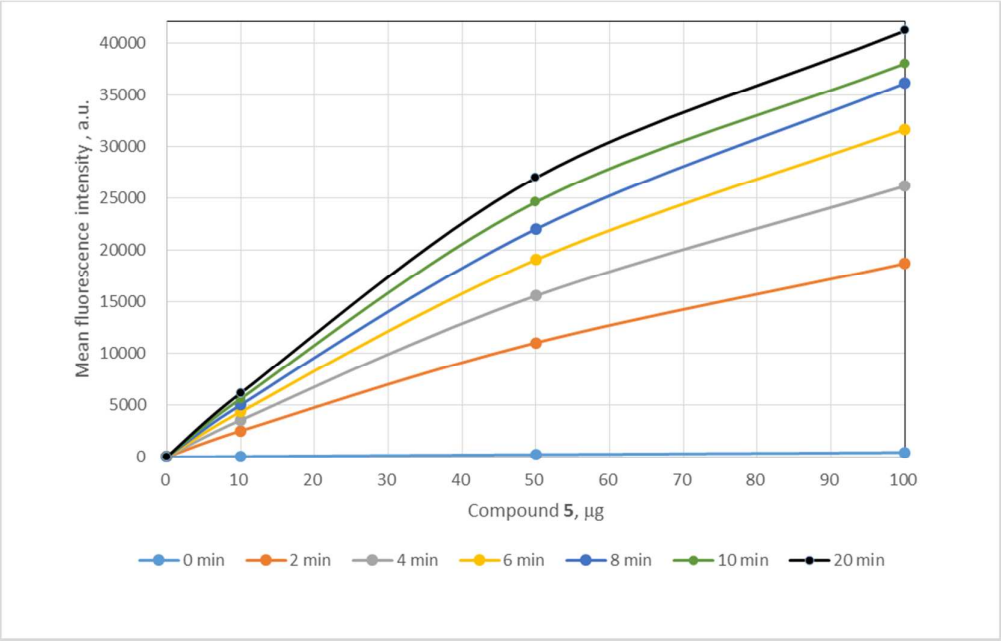

Figure 15. An increase of the fluorescent signal as a result of its accumulation during 2, 4, 6, 8, 10 or 20 min for different quantities of compound **5** complexed with equimolar quantities of the fluorescent streptavidin-QD800 conjugate in an *in vitro* sandwich-type biochemical assay. The mean fluorescence intensities in the case of immediate signal recording (0 min of accumulation) in the presence of 10, 50, and 100 µg of compound **5** are 50, 220, and 420 a.u., respectively, which shows that the signal-to-noise ratios in assays employing QDs can be increased by more than two orders of magnitude.

As seen from Figure 16, accumulation of the signal from fluorogenic assays employing strepta-QD for revealing the (compound **5**)-MMP-2 complex during 10-20 min may result in an increase in the intensity of the signal by more than two orders of the magnitude, whereas the signals of all typical organic dyes recorded under exactly the same conditions are photobleached.

However, the most important fact is that the fluorescent signal from the assay employing strepta-QD obtained in the course of signal accumulation is more than two orders of magnitude stronger than that for the maximal signals that may be obtained for typical fluorogenic assays employing the best organic dyes under optimal conditions. This shows that the use of QD-based labels in typical fluorogenic assays is decisively advantageous.

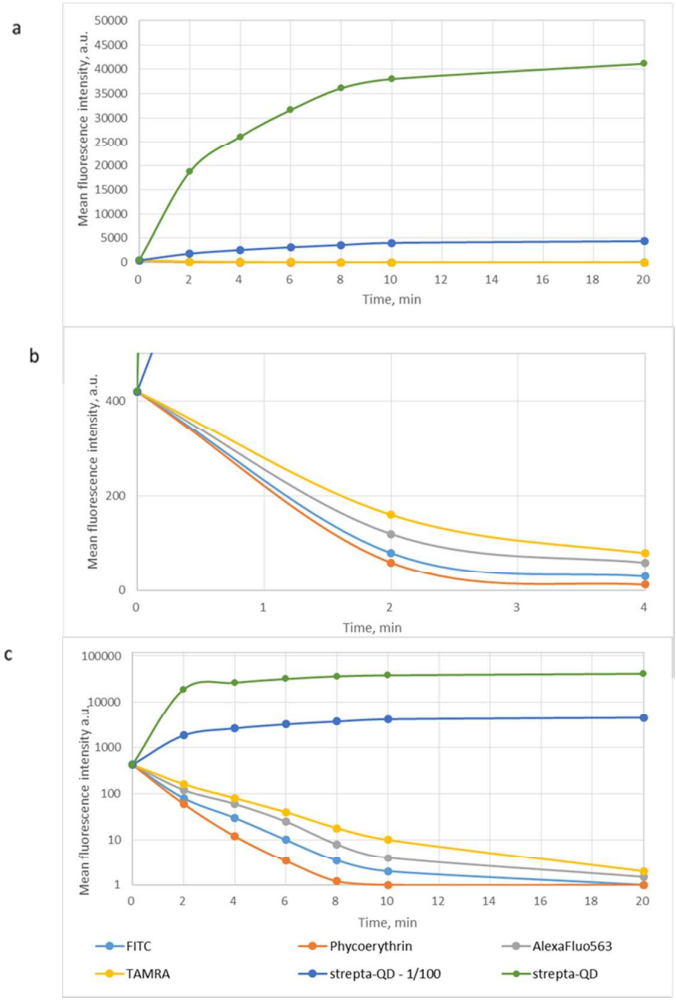

Figure 16. Comparative analysis of variations of fluorescent signals as a result of their accumulation at permanent signal-to-noise ratios for typical *in vitro* biochemical sandwich-like fluorogenic assays employing two different concentrations of the fluorescent streptavidin-QD800 conjugate and the most popular organic dyes.

Panels (a) and (b) show variations of the fluorescence signals from the model assays during signal accumulation for 20 min and 4 min, respectively. In Panel (a), the signals from organic

dyes are too weak to be visible in comparison with the signals from strepta-QDs at the equimolar concentration and even after a 1/100 dilution; in Panel (b), the signals from strepta-QD are strong and visible only in the initial period of signal accumulation.

Panel (c) shows the same data as in Panel (a) but on a demi-logarithmic scale. Here, the curves corresponding to the evolutions of the fluorescence signals from strepta-QDs and from different organic labels are visible in the same graph.

CONCLUSION

Proteolytic enzymes of the MMP family, in particular, MMP-2, are overexpressed during cancer pathological processes. Activated MMPs have been detected in tissues, plasma, serum, and urine of cancer patients at increased levels, they are also positively correlated with the severity of metastatic tumours.[75-77] Thus, MMPs can serve as selective and specific tumour markers for clinical applications.

Due to the unique potency to combine monitoring and therapy, nanoparticle-based techniques can provide an advantage over standard diagnostic and therapeutic tools with respect to disease diagnosis and monitoring, drug delivery and release. Moreover, nanoparticle-based diagnostic tools can be easily modified, combined, and improved to ensure multiplexed detection and advanced diagnostics sensitivity. Thus, nanoparticles (e.g., fluorescent nanocrystals or QDs) are considered a useful and indispensable tool for advanced clinical diagnostics, imaging, and therapeutic applications.[78]

In this study, a series of new MMP-inhibitors, ilomastat derivatives, have been prepared and subjected to preliminary biological evaluations in experiments with the main matrix metalloproteinases (MMP-1, MMP-2, MMP-9, MMP-13, and MMP-14). A systematic enzyme inhibition / selectivity study was carried out, with carboxylic acid serving as a zinc-binding group (ZBG), by introducing a phenyl group to the C2 carbon atom of the tryptophan indole ring and by incorporating alkylidene chains of different lengths at the P’1 position of the succinic

acid moiety. As a result of structure-activity relationship (SAR) studies, we have identified the most selective MMP-2 inhibitor with convenient inhibition potency (IC_{50} = 80 nM) and biotinylated it for the use in assays employing the QD-streptavidin conjugate for visualisation. The specific fluorescent complex of compound **5**-biotin/streptavidin-QD was tested and evaluated for MMP-2 inhibition in model *in vitro* sandwich-type analytic biochemical assays and compared with similar model assays employing typical organic dyes. The data show that the fluorogenic assays employing QDs allows the detection signal level to be increased by more than two orders of magnitude compared to typical organic dyes, thus paving the way to a considerable increase in the sensitivity of MMP detection in *in vitro* assays. The described ultrasensitive QD-based detection approach, exemplified here by MMP-2 detection, is by no means limited to it. Designing and using broad-spectrum inhibitors will allow this strategy to be efficiently modified for detecting both other MMPs and other hydrolytic enzymes for different substrates.

EXPERIMENTAL PROCEDURES

General synthesis methods and materials

Standard solvents were purchased from commercial sources and were dried by standard procedures and redistilled under N_2 prior to use. Reactions and products were routinely monitored by thin layer chromatography (TLC) on silica gel (KIESELGEL 60 PF254, Merck). HBTU and 2,4,6-collidine were purchased from commercial sources. Pure products were obtained by means of flash chromatography using Merck Geduran SI silica gel 60 (70-230 mesh ASTM). The melting points were determined using a Reichert Thermovar hot-stage apparatus and are uncorrected. The NIR-FT spectra (KBr or NaCl film) were measured using a Perkin-Elmer Spectrum BX FTIR instrument. The ^{1}H NMR (300 MHz) and ^{13}C NMR (75 MHz) spectra were recorded by means of a Bruker AC 300 spectrometer using TMS as an internal standard; the chemical shifts δ were expressed in ppm; the following abbreviations are used: singlet (s), doublet (d), doublet of doublets (dd), triplet (t), multiplet (m). Coupling constants J were expressed in hertz. Mass spectra were recorded by means of an MSQ ThermoFinnigan apparatus using the chemical ionization (CI) method. Electrospray ionization mass spectrometry experiments were carried out using a hybrid tandem quadrupole/time-of-flight (Q-TOF) instrument equipped with a pneumatically assisted electrospray (Z-spray) ion source (Micromass, Manchester, UK) operated in the positive mode. Optical rotations were measured on a Perkin-Elmer 241 polarimeter (Na lamp, $\lambda = 589$ nm).

Synthesis procedures

*(S)-ethyl3-(1H-indol-3-yl)-2-(2,2,2-trifluoroacetamido)propanoate **7***

L-tryptophan (5.0 g, 24.5 mmol) was dissolved in absolute ethanol (80 mL). Thionyl chloride (3.6 mL, 2 equiv, 48.9 mmol) was added dropwise during 15 min. The mixture was refluxed for 3.5 h; then, the solvent was evaporated. The white solid was dissolved in EtOAc, the organic phase was washed with an aqueous solution of $NaHCO_3$ (5%) and then dried over $MgSO_4$. After filtration and concentration of the solvent, a slightly yellow oil was obtained. Then, CH_2Cl_2 (110

mL), triethylamine (3.4 mL, 1 equiv, 24.5 mmol), and trifluoroacetic anhydride (8.2 mL, 2.4 equiv, 58.6 mmol) were added at 0°C. The mixture was stirred at room temperature overnight. The solvent was evaporated; the crude product was purified by flash chromatography (Cyclohexane/CH_2Cl_2: 40/60) to afford the white solid of compound **7** (5.6 g, 72%). mp: 117-119°C. $[\alpha]^{21}_D$ -21 (c 1.13, DMSO). ^{1}H NMR (DMSO-d_6, 300 MHz): δ 1.14 (t, 3H, J = 7.1 Hz), 3.20-3.35 (m, 2H), 4.12 (q, 2H, J = 7.1 Hz), 4.52-4.60 (m, 1H), 7.02-7.10 (m, 2H), 7.18 (s, 1H), 7.37 (d, 1H, J = 8.1 Hz), 7.55 (d, 1H, J = 7.8 Hz), 9.95 (d, 1H, J = 7.5 Hz), 10.92 (s, 1H). ^{13}C NMR (DMSO-d_6, 75 MHz): δ 14.1, 26.2, 54.0, 61.3, 109.4, 110.6, 111.7, 114.4, 118.2, 118.4, 118.7, 121.3, 122, 124.0, 127.1, 136.3, 155.9, 156.4, 156.9, 157.4, 170.5. IR (KBr): ν (cm^{-1}) 3374, 3322, 1736, 1696, 1555, 1304, 1278, 1230, 1176, 1093, 1027, 873, 860, 741, 692. MS (CI): *m/z* 328.96 [$M^{+\cdot}$] (100), 311 (14), 283 (15), 255 (25), 242 (23), 238 (59). Anal. Calcd for $C_{15}H_{15}N_2O_3F_3$: C 54.88, H 4.61, N, 8.53%. Found: C 54.64, H 4.74, N 8.38%.

(S)-ethyl 3-(2-phenyl-1H-indol-3-yl)-2-(2,2,2-trifluoroacetamido)propanoate ***8***

N-bromosuccinimide (54 mg, 0.3 mmol) was added to a suspension of α-*N*-(trifluoroacety1)-*L*-tryptophan ethyl ester **7** (0.1 g, 0.3 mmol) in CCl_4 (2 mL). The mixture was refluxed for 30 min under nitrogen, and the solvent was evaporated *in vacuo*. The filtrate was purified by flash chromatography (Petroleum ether/EtOAc: 9/1) to afford a brominated compound (118 mg, 96%). mp: 134-137°C. $[\alpha]^{21}_D$ -14 (c 1.41, DMSO). ^{1}H NMR ($CDCl_3$, 300 MHz): δ 1.22 (t, 3H, J = 7.1 Hz), 3.29-3.35 (m, 2H), 4.08-4.24 (m, 2H), 4.91 (dd, 1H, J = 13.8 Hz, J = 5.8 Hz), 6.99 (d, 1H, J = 7.1 Hz), 7.09-7.20 (m, 2H), 7.25 (d, 1H, J = 7.4 Hz), 7.46 (d, 1H, J = 7.7 Hz), 8.35 (s, 1H). ^{13}C NMR ($CDCl_3$, 75 MHz): δ 13.8, 27.3, 52.9, 62.5, 109.0, 109.6, 109.8, 110.7, 113.6, 117.4, 117.7, 120.5, 121.2, 122.8, 127.5, 136.0, 156.0, 156.5, 157.0, 157.5, 170.2. IR (KBr): ν (cm^{-1}) 3339, 1727, 1701, 1555, 1450, 1419, 1278, 1194, 1164, 1027, 873, 741, 723, 648. Anal. Calcd for $C_{15}H_{14}N_2O_3BrF_3$: C 44.25, H 3.47, N 6.88%. Found: C 44.41, H 3.34, N 6.78%.

Phenylboronic acid (52 mg, 1.5 equiv, 0.42 mmol) was dissolved in a mixture of toluene and ethanol (1/1) (4 mL), the brominated compound (115 mg, 0.28 mmol), $NaHCO_3$ (47 mg, 2 equiv,

0.56 mmol) dissolved in pure water (1 mL), and LiCl (36 mg, 3 equiv, 0.84 mmol); finally, catalyst $Pd(PPh_3)_4$ (32 mg, 0.1 equiv, 0.028 mmol) was added. The yellow solution was stirred under reflux for 2 h. The red mixture was concentrated; then, CH_2Cl_2 and an aqueous solution of $NaHCO_3$ (10%) were added. The aqueous phase was extracted twice with CH_2Cl_2. The organic phases were collected, dried over $MgSO_4$, filtered, and concentrated. The crude product was purified by flash chromatography (petroleum ether/EtOAc: 9/1) to afford compound **8** (105 g, 92%). mp: 172-174°C. $[\alpha]^{21}_D$ -10.5 (c 0.84, DMSO). ^{1}H NMR ($CDCl_3$, 300 MHz): δ 1.02 (t, 3H, *J* = 7.1 Hz), 3.56-3.62 (m, 3H), 3.91-3.97 (m, 1H), 4.81 (dd, 1H, *J* = 13.6 Hz, *J* = 5.8 Hz), 6.68 (d, 1H, *J* = 7.4 Hz), 7.12-7.57 (m, 9H), 8.22 (s, 1H). ^{13}C NMR ($CDCl_3$, 75 MHz): δ 13.7, 26.5, 53.4, 61.9, 105.6, 109.0, 111.0, 113.0, 117.0, 118.5, 120.2, 121.0, 122.7, 128.2, 128.3, 128.9, 129.0, 129.1, 132.5, 135.6, 136.3, 155.1, 155.7, 156.3, 156.9, 170.2. IR (KBr): ν (cm^{-1}) 3374, 3286, 1753, 1705, 1555, 1450, 1278, 1203, 1172, 1018, 877, 745, 697. MS (CI): *m/z* [M+1] 405.29 (100), 405 (60), 339 (15), 218 (20), 206 (15). Anal. Calcd for $C_{21}H_{19}N_2O_3F_3$: C 62.37, H 4.74, N 6.93%. Found: C 62.18, H 4.66, N 6.82%.

(S)-ethyl3-(1-(3-tert-butoxy-3-oxopropyl)-2-phenyl-1H-indol-3-yl)-2-(2,2,2-trifluoroacetamido)propanoate ***9***

*t*BuOK (107 mg, 1.3 equiv, 0.95 mmol) was added to a solution of compound **8** (296 mg, 0.73 mmol) in THF (5 mL); the solution was stirred for 15 min under nitrogen. Then, *tert*-butylacrylate (1 mL) was added to the solution dropwise. The reaction mixture was incubated upon heating to reflux for 3.5 h. The mixture was diluted with a solution of saturated NH_4Cl and extracted with EtOAc. The organic phase was dried over $MgSO_4$ and filtered, and the solvent was evaporated. The crude product was purified by flash chromatography (petroleum ether/EtOAc: 85/15) to afford compound **9** (351 mg, 90%). mp: 84-86°C. $[\alpha]^{21}_D$ -2.4 (c 0.5, MeOH). ^{1}H NMR ($CDCl_3$, 300 MHz): δ 1.08 (t, 3H, *J* = 7.1 Hz), 1.32 (s, 9H), 2.37-2.43 (m, 2H), 3.33 (ddd, 2H, *J* = 5.7 Hz, *J* = 14.7 Hz, *J* = 20.4 Hz), 3.74-3.80 (m, 1H), 3.98-4.04 (m, 1H), 4.25-4.30 (m, 2H), 4.71 (dd, 1H, *J* = 6.1 Hz, *J* = 13.9 Hz), 6.51 (d, 1H, *J* = 7.8 Hz), 7.15-7.61

(m, 9H). ^{13}C NMR ($CDCl_3$, 75 MHz): δ 13.7, 26.6, 26.8, 27.8, 35.8, 39.5, 53.2, 61.8, 81.0, 106.7, 109.9, 117.2, 118.4, 118.5, 119.9, 120.0, 121.1, 122.3, 127.8, 128.8, 129.0, 130.4, 130.9, 136.0, 138.9, 155.0, 155.9, 156.8, 157.7, 170.1, 170.1. IR (NaCl): ν (cm^{-1}) 3400, 3322, 2976, 2925, 1723, 1540, 1462, 1361, 1207, 1155, 1018, 739, 700. HRMS (ESI): *m/z* calcd for $C_{28}H_{32}N_2O_5F_3$ 533.2263, found 533.2257 (-1.2 ppm). Anal. Calcd for $C_{28}H_{31}N_2O_5F_3$: C 63.09, H 5.82, N 5.25%. Found: C 62.99, H 6.00, N 5.41%.

(S)-tert-butyl 3-(3-(2-amino-3-(methylamino)-3-oxopropyl)-2-phenyl-1H-indol-1-yl)propanoate ***10***

A solution of compound **9** (304 mg, 0.57 mmol) in absolute ethanol (2.3 mL) and aqueous methylamine (40%) (2.3 mL) was stirred at room temperature overnight. The solvent was evaporated, and the crude product was diluted in CH_2Cl_2. The organic phase was washed twice with an aqueous solution of HCl (5%). The collected acid phases were then alkalized with an aqueous solution of $NaHCO_3$ (10%) to reach pH 8. The aqueous phase was extracted with CH_2Cl_2, dried over $MgSO_4$, and filtered. Evaporation of the solvent gave white foam (191 mg, 80%). $[\alpha]^{21}_D$ +9.2 (c 0.5, MeOH). ^{1}H NMR ($CDCl_3$, 300 MHz): δ 1.31 (s, 9H), 2.39-2.44 (m, 2H), 2.68-2.76 (m, 4H), 3.40-3.45 (m, 1H), 3.60-3.64 (m, 1H), 4.26-4.31 (m, 2H), 7.13-7.54 (m, 9H), 7.73 (d, 1H, *J* = 7.7 Hz). ^{13}C NMR ($CDCl_3$, 75 MHz): δ 25.7, 27.8, 29.9, 35.8, 39.5, 55.3, 81.0, 109.7, 109.8, 119.3, 119.7, 122.1, 127.6, 128.6, 128.8, 130.5, 131.4, 136.1, 138.9, 170.1, 175.1. IR (NaCl): ν (cm^{-1}) 3379, 3302, 2914, 1723, 1659, 1527, 1462, 1364, 1150, 845, 742, 703. HRMS (ESI): *m/z* calcd for $C_{25}H_{32}N_3O_3$ 422.2444, found 422.2449 (1.3 ppm). Anal. Calcd for $C_{25}H_{31}N_3O_3.H_2O$: C 68.33, H 7.06, N 9.56%. Found: C 68.21, H 7.34, N 9.53%.

(S,E)-allyl 3-(3-(1-(3-tert-butoxy-3-oxopropyl)-2-phenyl-1H-indol-3-yl)-1-(methylamino)-1-oxopropan-2-ylcarbamoyl)tridec-3-enoate ***12***

HBTU (300 mg, 1.5 equiv, 0.79 mmol) and 2,4,6-collidine (141 μL, 2 equiv, 10 mmol) were added to a solution of compound **10** (157 mg, 0.53 mmol) in dry CH_2Cl_2 (20 mL). The reaction mixture was stirred for 1 h at room temperature; then, a solution of compound **11** (223 mg, 0.53

mmol) in dry CH_2Cl_2 (20 mL) was added, and the solution was stirred overnight at room temperature. The solvent was evaporated, and the crude product was purified by flash chromatography (CH_2Cl_2/MeOH: 99/1, 98/2) to afford compound **12** (304 g, 82%). $[\alpha]^{21}_D$ -4.2 (c 0.5, MeOH). ^{1}H NMR ($CDCl_3$, 300 MHz): δ 0.89 (t, 3H, *J* = 7.1 Hz), 1.24-1.31 (m, 23H), 2.01-2.06 (m, 2H), 2.38 (t, 2H, *J* = 7.7 Hz), 2.60 (d, 3H, *J* = 4.8 Hz), 3.13-3.41 (m, 4H), 4.29 (t, 2H, *J* = 7.5 Hz), 4.50-4.52 (m, 2H), 4.62 (dd, 1H, *J* = 7.3 Hz, *J* = 14.4 Hz), 5.16-5.23 (m, 2H), 5.79-5.85 (m, 2H), 5.96 (t, 1H, *J* = 7.3 Hz), 6.47 (d, 1H, *J* = 7.3 Hz), 7.17-7.50 (m, 8H), 7.84 (d, 1H, *J* = 7.6 Hz). ^{13}C NMR ($CDCl_3$, 75 MHz): δ 14.1, 22.6, 26.2, 27.2, 27.8, 28.4, 28.5, 29.2, 29.3, 29.4, 29.6, 31.8, 32.5, 35.7, 39.6, 53.8, 65.5, 81.0, 109.0, 109.8, 118.3, 119.4, 120.1, 122.2, 127.8, 128.6, 128.8, 129.4, 130.4, 131.0, 131.7, 136.2, 138.2, 138.6, 168.6, 170.1, 170.9, 171.4. IR (NaCl): ν (cm^{-1}) 3405, 3317, 2925, 2852, 1726, 1659, 1625, 1511, 1462, 1364, 1323, 1253, 1152, 990, 922, 742, 700. HRMS (ESI): *m/z* calcd for $C_{42}H_{57}N_3O_6Na$ 722.4145, found 722.4135 (-1.5 ppm). Anal. Calcd for $C_{42}H_{57}N_3O_6.H_2O$: C 70.29, H 7.95, N 5.85%. Found: C 70.19, H 8.20, N 6.89%.

*(S,E)-3-(3-(2-(2-(2-(allyloxy)-2-oxoethyl)dodec-2-enamido)-3-(methylamino)-3-oxopropyl)-2-phenyl-1H-indol-1-yl)propanoic acid **13***

TFA (4 mL) was added to a solution of compound **12** (300 mg, 0.42 mmol) in dry CH_2Cl_2 (10 mL), and the mixture was sequentially stirred for 30 min at 0°C and for 30 min at room temperature. After evaporation, an orange oil was obtained (276 mg, 100%). ^{1}H NMR ($CDCl_3$, 300 MHz): δ 0.89 (t, 3H, *J* = 6.5 Hz), 1.24-1.41 (m, 14H), 2.03-2.10 (m, 2H), 2.46-2.60 (m, 5H), 3.17-3.31 (m, 4H), 4.33 (t, 2H, *J* = 7.5 Hz), 4.50 (d, 2H, *J* = 5.5 Hz), 4.67-4.69 (m, 1H), 5.17-5.28 (m, 2H), 5.78-5.83 (m, 1H), 6.15 (t, 1H, *J* = 6.8 Hz), 6.56 (s, 1H), 7.13-7.65 (m, 10H), 9.8 (s, 1H). ^{13}C NMR ($CDCl_3$, 75 MHz): δ 14.0, 22.6, 26.7, 26.9, 28.3, 28.6, 29.2, 29.3, 29.4, 29.6, 31.8, 32.5, 34.3, 39.5, 54.5, 65.9, 107.9, 109.7, 118.6, 118.7, 120.2, 122.5, 127.8, 127.9, 128.9, 130.3, 130.6, 131.4, 135.9, 138.8, 141.3, 170.0, 171.6, 172.9, 172.9. IR (NaCl): ν (cm^{-1}) 3307,

3054, 2925, 2852, 1731, 1661, 1635, 1527, 1465, 1408, 1359, 1271, 1196, 1176, 1137, 987, 925, 742, 716, 700. HRMS (ESI): *m/z* calcd for $C_{38}H_{50}N_3O_6$ 644.3700, found 644.3702 (0.4 ppm).

Tert-butyl 3-(5-(2-oxo-hexahydro-*1H-thieno[3,4-d]imidazol-4-yl)pentanamido) *propylcarbamate* ***16***

HBTU (232 mg, 1.5 equiv, 0.61 mmol) and 2,4,6-collidine (110 µL, 2 equiv, 0.81 mmol) were added to a solution of biotin **15** (100 mg, 0.41 mmol) in dry DMF (3 mL). The reaction mixture was stirred for 1 h at room temperature; then, a solution of compound **14** (107 mg, 1.5 equiv, 0.61 mmol) in dry CH_2Cl_2 (3 mL) was added, and the mixture was stirred overnight at room temperature. The solvent was evaporated, and the crude product was purified by flash chromatography (CH_2Cl_2/MeOH: 9/1, 8/2) to afford compound **16** (121 mg, 74%). mp: 93-95°C. $[\alpha]^{21}_D$ +47.8 (c 0.5, MeOH). ^{1}H NMR (DMSO-d_6, 300 MHz): δ 1.25-1.53 (m, 17H), 2.05 (t, 2H, J = 7.3 Hz), 2.56-2.60 (m, 1H), 2.83 (dd, 1H, J = 5.1 Hz, J = 12.4 Hz), 2.89 (dd, 2H, J = 6.2 Hz, J = 12.8 Hz), 3.02 (dd, 2H, J = 6.7 Hz, J = 12.9 Hz), 3.10-3.12 (m, 1H), 4.11-4.15 (m, 1H), 4.29-4.33 (m, 1H), 6.38 (s, 1H), 6.45 (s, 1H), 6.79 (t, 1H, J = 5.2 Hz), 7.77 (t, 1H, J = 5.4 Hz). ^{13}C NMR ($CDCl_3$, 75 MHz): δ 25.3, 27.8, 27.8, 28.1, 29.4, 35.6, 35.9, 37.0, 40.1, 55.3, 59.9, 61.6, 79.2, 156.7, 164.0, 174.1. IR (NaCl): ν (cm^{-1}) 3297, 2925, 1687, 1524, 1457, 1361, 1276, 1248, 1165, 842. HRMS (ESI): *m/z* calcd for $C_{18}H_{32}N_4O_4SNa$ 423.2042, found 423.2035 (-1.7 ppm). Anal. Calcd for $C_{18}H_{32}N_4O_4S.2H_2O$: C 49.54, H 7.33, N 12.84, S 7.32%. Found: C 49.40, H 7.66, N 13.68, S 6.78%.

N-(3-aminopropyl)-5-(2-oxo-hexahydro-1H-thieno[3,4-d]imidazol-4-yl)pentanamide ***17***

TFA (1 mL) was added to a solution of compound **16** (95.5 mg, 0.24 mmol) in dry CH_2Cl_2 (2 mL), and the mixture was sequentially stirred for 30 min at 0°C and for 30 min at room temperature. After evaporation, an orange oil was obtained (144 mg, 100%). ^{1}H NMR ($CDCl_3$, 300 MHz): δ 1.41-1.52 (m, 2H), 1.58-1.69 (m, 4H), 1.83-1.88 (m, 2H), 2.19-2.27 (m, 2H), 2.72-2.96 (m, 4H), 3.15-3.21 (m, 1H), 3.28-3.38 (m, 2H), 4.32-4.36 (m, 1H), 4.52-4.58 (m, 1H). ^{13}C NMR ($CDCl_3$, 75 MHz): δ 25.0, 26.8, 27.6, 27.8, 35.0, 35.3, 36.5, 40.0, 55.3, 60.1, 61.9, 164.2,

175.5. IR (NaCl): ν (cm^{-1}) 3291, 2919, 2852, 1661, 1457. HRMS (ESI): *m/z* calcd for $C_{13}H_{25}N_4O_2S$ 301.1620, found 301.1691.

(E)-allyl 3-((S)-1-(methylamino)-1-oxo-3-(1-(3-oxo-3-(3-(5-(2-oxo-hexahydro-1H-Thieno[3,4-d]imidazol-4-yl)pentanamido)propylamino)propyl)-2-phenyl-1H-indol-3-yl)propan-2-ylcarbamoyl)tridec-3-enoate ***18***

HBTU (108 mg, 1.2 equiv, 0.28 mmol) and 2,4,6-collidine (47 μL, 1.5 equiv, 0.35 mmol) were added to a mixture of compound **13** (0.23 mmol) in dry CH_2Cl_2 (2 mL) and DMF (1 mL). The reaction mixture was stirred for 1 h at room temperature; then, a solution of compound **17** (0.23 mmol) in dry CH_2Cl_2 (2 mL) and 2,4,6-collidine (47 μL, 1.5 equiv, 0.35 mmol) were added, and the solution was stirred overnight at room temperature. The solvents were evaporated. The mixture was diluted with EtOAc (2 mL). The organic phase was washed sequentially with a solution of citric acid (1 N), a solution of $NaHCO_3$ (1 N), and a solution of NaCl and dried over $MgSO_4$. After filtration and evaporation, the crude product was purified by flash chromatography (CH_2Cl_2/MeOH: 9/1, 8/2) to afford compound **18** (83 mg, 38% over two steps). mp: 86-88°C. $[\alpha]^{21}_D$ +9.8 (c 0.5, MeOH). ^{1}H NMR (DMSO-d_6, 300 MHz): δ 0.87 (t, 3H, J = 6.0 Hz), 1.27-1.52 (m, 22H), 2.02-2.09 (m, 4H), 2.28-2.31 (m, 2H), 2.42 (d, 3H, J = 4.4 Hz), 2.56-2.60 (m, 1H), 2.79-3.29 (m, 10H), 4.12-4.19 (m, 3H), 4.28-4.47 (m, 4H), 5.19 (ddd, 2H, J = 1.1 Hz, J = 17.3 Hz, J = 18.2 Hz), 5.79-5.85 (m, 1H), 6.25 (t, 1H, J = 7.2 Hz), 6.38 (s, 1H), 6.44 (s, 1H), 7.03-7.19 (m, 2H), 7.40-7.83 (m, 11H). ^{13}C NMR (DMSO-d_6, 75 MHz): δ 14.2, 22.3, 25.5, 25.8, 27.8, 28.2, 28.4, 28.9, 29.1, 29.2, 31.5, 35.4, 36.0, 36.3, 36.5, 36.5, 39.9, 40.2, 54.8, 55.6, 59.3, 61.2, 64.6, 109.2, 110.1, 117.5, 119.2, 119.3, 121.5, 128.0, 128.7, 129.1, 130.8, 131.3, 132.7, 135.9, 138.2, 138.3, 162.9, 167.3, 169.5, 170.4, 171.7, 172.1. IR (NaCl): ν (cm^{-1}) 3421, 3302, 2919, 2852, 1695, 1653, 1545, 1532, 1462, 1354, 1325, 1263, 1173, 842, 739. HRMS (ESI): *m/z* calcd for $C_{51}H_{71}N_7O_7SNa$ 948.5033, found 948.5041 (0.8 ppm). Anal. Calcd for $C_{51}H_{71}N_7O_7S.6H_2O$: C 59.24, H 6.87, N 9.48, S 3.09%. Found: C 59.18, H 7.04, N 10.17, S 4.14%.

(E)-3-((S)-1-(methylamino)-1-oxo-3-(1-(3-oxo-3-(3-(5-(2-oxo-hexahydro-1H-thieno[3,4-d]imidazol-4-yl)pentanamido)propylamino)propyl)-2-phenyl-1H-indol-3-yl)propan-2-ylcarbamoyl)tridec-3-enoic acid ***5***

Allyl ester **18** (64 mg, 0.07 mmol) was dissolved in THF (2 mL) in a nitrogen atmosphere and supplied with a catalyst ($Pd(PPh_3)_4$, 0.1 equiv) and morpholine (18.6 µL, 3.1 equiv, 0.21 mmol) in the dark. After incubation for 30 min, the solvent was evaporated. The organic phase was filtered through the Celite® filter agent, and the resultant solution was concentrated *in vacuo*. The concentrate was purified by silica gel column chromatography with the solvent CH_2Cl_2/MeOH: 7/3 to afford acid compound **5** as a white solid (44 mg, 72%). mp: 103-105°C. $[\alpha]^{21}_D$ +21.2 (c 0.5, MeOH). ^{1}H NMR (DMSO-d_6, 300 MHz): δ 0.87 (t, 3H, J = 6.8 Hz), 1.26-1.49 (m, 22H), 1.99-2.09 (m, 4H), 2.29-2.41 (m, 2H), 2.42 (d, 3H, J = 4.4 Hz), 2.77-3.10 (m, 11H), 4.11-4.40 (m, 5H), 6.14 (t, 1H, J = 7.2 Hz), 6.37 (s, 1H), 6.45 (s, 1H), 6.99-7.14 (m, 2H), 7.41-7.65 (m, 8H), 7.89 (t, 1H, J = 4.8 Hz), 8.06 (d, 1H, J = 7.8 Hz), 8.41 (bs, 1H). ^{13}C NMR (DMSO-d_6, 75 MHz): δ 14.2, 22.3, 25.5, 25.9, 27.8, 28.2, 28.4, 28.6, 28.9, 29.1, 31.5, 35.4, 35.6, 36.0, 39.9, 40.2, 54.5, 55.6, 59.3, 61.2, 109.0, 110.3, 119.0, 119.4, 121.4, 127.7, 128.6, 131.0, 131.4, 131.5, 136.1, 136.4, 138.6, 162.9, 168.5, 170.1, 172.0, 172.3, 173.5. IR (NaCl): ν (cm^{-1}) 3266, 2919, 2852, 2356, 2330, 1651, 1643, 1555, 1542, 1465, 1457, 1359, 1261, 1106, 742. HRMS (ESI): *m/z* calcd for $C_{48}H_{67}N_7O_7SNa$ 908.4720, found 908.4724 (0.3 ppm). Anal. Calcd for $C_{48}H_{67}N_7O_7S.4H_2O$: C 60.18, H 7.00, N 10.24, S 3.34%. Found: C 60.91, H 7.82, N 10.50, S 2.90%.

Molecular modelling

The AutoDock 4.0 software was used to perform the computational molecular docking. The AutoDockTools package was employed to prepare the input files necessary for the docking procedures and to analyse the results of docking. Figures were constructed using the PyMOL software (DeLano, W. L. 2002. PyMol Molecular Graphics System, Palo Alto, CA. http://www.pymol.org).

Initial data on MMPs and ligands

The structures from the Protein Data Bank (PDB) entries 1CK7 (for MMP-2)[79] and 1GKC (for MMP-9)[80] were used for docking simulations. While MMP atoms and the zinc ion in the catalytic site were retained, all the other atoms were removed. Residues 31–109 corresponding to the pro-domain prohibiting the MMP-2 proteolytic activity have been also removed. The protonation states of all ionisable residues were computed using the PROPKA software.[81,82] The MMP side chains were kept fixed for all the docking computations. Ligands were built using the Marvin software (Marvin 5.3.2, 2010, ChemAxon: http://www.chemaxon.com). The AutoDock module AutoTors was used to determine the torsion angles of the ligands. All the flexible torsions except amide bonds were allowed to rotate during the docking stage.

Molecular docking simulations and calculations

Affinity grid maps were calculated for each atom type constituting MMP-2 with the use of the AutoGrid software. Grid maps were centred on the MMP catalytic site, with 126 x 126 x 126 grid points and spacings of 0.291 and 0.225 Å between the grid points for MMP-2 and MMP-9, respectively. Mehler and Solmajer's[83] distance-dependent dielectric permittivity was used for the calculations of the electrostatic grid maps. Random starting positions on the entire protein surface and random orientations and torsions were used for all ligands. The AutoDock software, version 4.0, was used for docking computations, with a Lamarckian genetic algorithm.[62,63] Each docking experiment was performed with four runs constituted of a series of 250 simulations. Each docking simulation was carried out with an initial population of 250 individuals, a maximum number of 2,500,000 energy evaluations and a maximum number of 27,000 generations. The pseudo-Solis and Wets modification methods were used with default parameters. The docked conformations of the ligands were clustered with a root mean square deviation (RMSD) cut-off of 0.5 Å.

Biological evaluations

Inhibition studies

The quenched fluorogenic substrates DNP-Pro-Cha-Gly-Cys(Me)-His-Ala-Lys(*N*-Me-Abz)-NH_2 for MMP-1 or MMP-9 inhibition (where DNP is 2,4-dinitrophenyl; Cha is β-cyclohexylalanyl; Abz is 2-aminobenzoyl(antraniloyl)) were purchased from Calbiochem (VWR, Strasbourg, France), Mca L-Pro-Leu-Gly-Leu-Dpa-Ala-Arg-NH_2 for MMP-2, MMP-13, or MMP-14 inhibition (where Mca is (7-methoxycoumarin-4-yl); Dpa is [*N*-3-(2,4-dinitrophenyl)-*L*-2,3-diaminopropionyl]) and 6-(7-nitro-benzo[1,2,5]oxodiazol-4-ylamino)-hexanoyl-Arg-Pro-Lys-Pro-Leu-Ala-Nva-Trp-Lys(7 dimethylaminocoumarin-4-yl)NH_2 for MMP-3 inhibition were from Bachem (Weil am Rhein, Germany). The Dye Quenched fluorogenic substrate (DQ Gelatin) and EnzCheck Gelatinase/Collagenase assays were purchased from Life Technologies (USA).

Human recombinant pro-MMP-1, pro-MMP-2, pro-MMP-9, pro-MMP-13, and catalytic domains of MT1-MMP were obtained from Calbiochem. The pro-enzymes (pro-MMP-2 or pro-MMP-9) were freshly activated with 1–4 mM *p*-aminophenylmercuric acetate (APMA, Sigma-Aldrich, Saint Quentin Fallavier, France) at 37°C for 1–2 h. Fluorescent conjugates of streptavidin with QDs were purchased from Life Technologies (USA).

In vitro fluorogenic substrate digestion assay

Briefly, 1 nM of MMP-1, 0.95 nM of MMP-2, 0.89 nM of MMP-9, 0.6 nM of MMP-13, and 3.1 nM of MMP-14 catalytic domain were incubated with increasing concentrations of the synthetic compounds (from 1 to 5000 nM). Assays were initiated by adding the respective fluorogenic substrate (1–10 nM). The fluorescence was monitored with a Perkin Elmer HT Soft 7000 plus spectrofluorimeter (Perkin Elmer, Courtaboeuf, France). Upon cleavage of the fluorogenic peptide by MMP, the initial rate of the peptide hydrolysis in the absence (Vo) or presence (Vi) of the synthetic molecule was determined. The IC_{50} was calculated after plotting Vi/Vo as a function of the synthetic molecule concentration by fitting with a non-linear regression (Grafit Computer software, R. Leatherbarrow, Erithacus Software).

MMP-2 proteolytic activity measurement

MMP-2 activity was estimated in EnzCheck Gelatinase/Collagenase standard commercial assays based on digestion of an internally quenched fluorescent substrate with an activated enzyme according to the manufacturer's protocol. Briefly, 0.35–2 μg of recombinant MMP-2 was first pre-activated with 2.5 mM APMA in an activation buffer (50 mM Tris-HCl pH 7.5, 150 mM NaCl, 20 mM $CaCl_2$, 0.01% Tween-20) during 1.5 h at 37°C. Upon activation, 0–100 ng of MMP-2 was mixed with 50 μg/mL Dye Quenched substrate (DQ Gelatin) in a total volume of 200 μL of the activating buffer in a black non-treated 96-well plate. The samples were incubated at room temperature while protected from light for 2 to 24 h. The activity of MMP-2 was measured fluorimetrically in a fluorescence microplate reader (Infinite M200 Pro, Tecan, Switzerland). Since the reaction of quenched fluorescent substrate digestion with the activated enzyme is continuous, fluorescence was measured at multiple time points: 0, 20, 40, 60, 80, 100, 120 min, *etc*. The fluorescence of digested products of the Dye Quenched fluorogenic substrate (DQ gelatin) was induced at 488 nm and measured at 525 nm in a fluorescence microplate reader equipped with two monochromatic scanners. Background fluorescence was corrected by subtracting the value derived from no-enzyme substrate control.

This protocol was also employed for the detection of compound **5** (the enzyme inhibitor).

In this case, 50 ng of activated MMP-2 was pre-mixed with 0–50 μg of compound **5** preliminarily dissolved in DMSO in a total volume of 100 μL of the activating buffer. This enzyme–inhibitor mixture was supplemented with 50 μg/mL Dye Quenched fluorogenic substrate (DQ gelatin) in a total volume of 200 μL, and the inhibited MMP-2 activity was measured fluorimetrically at different time points.

In vitro gelatinolytic assays

HT-1080 cells were grown to a density of 80% in a 24-well plate and treated with 12.5 μg/mL concanavalin A overnight to convert pro-MMP-2 into active MMP-2. Cells were pre-incubated with or without effectors (100 μM **4k**, 10 μM ilomastat (Galardin®) for 1 h and then with DQ gelatin (500 ng/300 μL per well). Fluorescence was measured at 525 nm.

In vitro invasion assay was performed in modified Boyden chambers (tissue culture treated; diameter, 6.5 mm; pore size, 8 μm; Greiner-One, Courtaboeuf, France). $5x10^4$ HT-1080 cells were suspended in serum-free DMEM with 4.5 g/L glucose containing 0.2% (w/v) BSA and seeded onto membranes coated with Matrigel® (20 μg/well). The lower compartment was filled with DMEM supplemented with 10% (v/v) FBS and 2% (w/v) BSA. After a 6-h incubation period, the cells were fixed with methanol and stained with crystal violet for 15 min. The cells remaining on the upper face of the membrane were scraped. Crystal violet staining of the migrating cells (on the lower face) was eluted with 10% (v/v) acetic acid, and absorbance was read at 560 nm.

Quantum dot-based assays

The streptavidin-coated QDs used in this study were purchased from Invitrogen Corporation, and the optical and physical properties are summarized in the electronic supporting information.

Dot-blotting

The formation of the complex of biotinylated compound **5** with streptavidin-QD conjugate was visualized using the dot-blot detection technique. Briefly, different amounts (0–20 μg) of biotinylated compound **5** dissolved either in methanol or in DMSO and supplied with PBS, pH 7.4, were applied onto a nitrocellulose or PVDF membrane in a total volume of 2 μL. The membrane was dried completely and blocked from non-specific binding of the fluorescent conjugate with 5% (w/v) non-fat dry milk in PBS (pH 7.4) containing 0.05% (v/v) Tween 20 during 1 h at room temperature. Then, the membrane was incubated with streptavidin-QD 565 nm fluorescent conjugate (1:100 dilution in PBS (pH 7.4) containing 0.5% (w/v) casein from bovine milk) during 40 min at room temperature and washed thoroughly three times with PBS (pH 7.4) containing 0.05% (v/v) Tween 20. The fluorescence of the inhibitor-QD complexes of different intensities was detected using a ChemiDoc MP Imaging system (Bio-Rad Laboratories, Inc., USA) equipped with a standard emission filter (605/50 filter).

Sandwich-type biochemical assay

The formation of a complete complex consisting of the enzyme MMP-2, biotinylated compound **5**, and fluorescent conjugate of streptavidin with QDs was performed by means of solid-state sandwich-type analytic biochemical assay. Briefly, APMA pre-activated MMP-2 enzyme or BSA protein control were adsorbed in a 96-well plate (Maxisorp Nunc, Thermo Fischer Scientific, Denmark) in PBS (pH 7.4) overnight at 4°C. Then, the wells were washed and blocked with 1.5% (w/v) casein in PBS (pH 7.4) with gentle shaking for 60 min at room temperature. Different amounts of biotinylated compound **5** (0–200 μg per well) were added into the wells, and the mixture was incubated with gentle shaking for 60 min at room temperature. Wells were then washed three times with PBS. Finally, MMP-2/compound **5** complexes and BSA controls were incubated with the fluorescent streptavidin-QD 800 nm conjugate (1:100 dilution in PBS (pH 7.4) containing 0.5% (w/v) casein) with gentle shaking for 40 min at room temperature. The wells were washed, after which QD fluorescence was induced at 488 nm and measured at 800 nm using a fluorescence microplate reader equipped with two monochromatic scanners.

AUTHOR INFORMATION

Corresponding Author's E-mail: *erika.bourguet@univ-reims.fr*

Postal address : Institut de Chimie Moléculaire de Reims, UMR 7312-CNRS, SFR Cap-Santé, UFR Pharmacie, Université de Reims Champagne-Ardenne 51 rue Cognacq-Jay, 51096 Reims Cedex, France. Phone: +33 326913733; fax : +33 326918029.

ACKNOWLEDGMENTS

I.N. and A.S. acknowledge support of the Agence Nationale de Recherche through the ICENAP project of the M-ERA.NET EU Programme, and the Ministry of Education and Science of the Russian Federation, contract no. 4.624.2014/K. Supports from the Université de Reims Champagne-Ardenne, SFR CAP-Santé, CNRS, Ministry of Higher Education and Research (MESR), Ligue contre le Cancer de la Marne, and EU-programme FEDER to the PlAneT CPER project are also acknowledged. Dr. W. Hornebeck is warmly thanked for his advices. Technical assistance of Mrs. M. Decarme and Dr. F. Antonicelli is gratefully acknowledged.

ABBREVIATIONS

APMA, *p*-aminophenylmercuric acetate; BRET, bioluminescence resonance energy transfer; BSA, Bovine serum albumin; CPP, cell penetrating peptide; DMF, dimethylformamide; DMSO, dimethyl sulfoxide; DMEM, Dulbecco's Modified Eagle's medium; FBS, Fetal bovine serum; FRET, Förster resonance energy transfer; HBTU, *O*-(Benzotriazol-1-yl)-*N,N,N′,N′*-tetramethyluronium hexafluorophosphate; IC_{50}, the half maximal inhibitory concentration; MMP(s), matrix metalloproteinase(s); MMPI(s), matrix metalloproteinase inhibitor(s); PBS, phosphate buffered saline; PVDF, polyvinylidene difluoride; QD(s), quantum dot(s), TFA, trifluoroacetic acid; THF, tetrahydrofuran; TLC, thin layer chromatography; ZBG, zinc binding group.

REFERENCES

(1) Xie, X. S., Yu, J., and Yang, W. Y. (2006) Living cells as test tubes. *Science 312(5771)*, 228-230.

(2) Elf, J., Li, G. W., and Xie, X. S. (2007) Probing transcription factor dynamics at the single-molecule level in a living cell. *Science 316(5828),* 1191-1194.

(3) Evanko, D. (2008) Watching single molecules in cells. *Nat. Methods 5(1)*, 25-25.

(4) Michalet, X., Pinaud, F. F., Bentolila, L. A., Tsay, J. M., Doose, S., Li, J. J., Sundaresan, G., Wu, A. M., Gambhir, S. S., and Weiss, S. (2005) Quantum dots for live cells, in vivo imaging, and diagnostics. *Science 307(5709),* 538-544.

(5) Gill, R., Zayats, M., and Willner, I. (2008) Semiconductor Quantum Dots for Bioanalysis. *Angew. Chem. Int. Ed. 47*, 7602-7625.

(6) Yum, K., Na, S., Xiang, Y., Wang, N., and Yu, M. F. (2009) Mechanochemical delivery and dynamic tracking of fluorescent quantum dots in the cytoplasm and nucleus of living cells. *Nano Lett. 9(5),* 2193-2198.

(7) Nabiev, I., Sukhanova, A., Artemyev, M., and Oleinikov, V. (2008) Fluorescent colloidal particles as detection tools in biotechnology systems. *Colloidal nanoparticles in biotechnology* (Elissari, A., Ed.), pp 133-168, Wiley & Sons Inc, London-Singapore.

(8) Prasad, P. N. (2004) Nanophotonics. Wiley, New York.

(9) Bilan, R., Fleury, F., Nabiev, I., and Sukhanova, A. (2015) Quantum dot surface chemistry and functionalization for cell targeting and imaging. *Bioconjug. Chem. 26(4),* 609-624.

(10) Karakoti, A. S., Shukla, R., Shanker, R., and Singh, S. (2015) Surface functionalization of quantum dots for biological applications. *Adv. Colloid. Interface Sci. 215*, 28-45.

(11) Delehanty, J. B., Bradburne, C. E., Boeneman, K., Susumu, K., Farrell, D., Mei, B. C., Blanco-Canosa, J. B., Dawson, G., Dawson, P. E., Mattoussi, H., et al. (2010) Delivering

quantum dot-peptide bioconjugates to the cellular cytosol: escaping from the endolysosomal system. *Integr. Biol. 2(5-6)*, 265-277.

(12) Jiang, T., Olson, E. S., Nguyen, Q. T., Roy, M., Jennings, P. A., and Tsien, R. Y. (2004) Tumor imaging by means of proteolytic activation of cell-penetrating peptides. *Proc. Natl. Acad. Sci. U.S.A. 101(51),* 17867-17872.

(13) Jańczewski, D., Tomczak, N., Han, M. Y., and Vancso, G. J. (2011) Synthesis of functionalized amphiphilic polymers for coating quantum dots. *Nat. Protoc. 6(10)*, 1546-1553.

(14) Sukhanova, A., Devy, J., Venteo, L., Kaplan, H., Artemyev, M., Oleinikov, V., Klinov, D., Pluot, M., Cohen, J. H., and Nabiev, I. (2004) Biocompatible fluorescent nanocrystals for immunolabeling of membrane proteins and cells. *Anal. Biochem. 324*, 60-67.

(15) Montenegro, J. M., Grazu, V., Sukhanova, A., Agarwal, S., de la Fuente, J. M., Nabiev, I., Greiner, A., and Parak, W. J. (2013) Controlled antibody/(bio-) conjugation of inorganic nanoparticles for targeted delivery. *Adv. Drug Deliv. Rev. 65(5)*, 677-688.

(16) Medintz, I. L., Uyeda, H. T., Goldman, E. R., and Mattoussi, H. (2005) Quantum dot bioconjugates for imaging, labelling and sensing. *Nat. Materials 4*, 435-446.

(17) Vaisanen, A., Tuominen, H., Kallioinen, M., and Turpeenniemi-Hujanen, T. (1996) Matrix metalloproteinase-2 (72 kD type IV collagenase) expression occurs in the early stage of human melanocytic tumour progression and may have prognostic value. *J. Pathol. 180*, 283-289.

(18) Overall, C. M., and Kleifeld, O. (2006) Tumour microenvironment - opinion: Validating matrix metalloproteinases as drug targets and anti-targets for cancer therapy. *Nature Rev. Cancer*, *6(3)*, 227-239.

(19) Bourguet, E., Sapi, J., Emmonard, H., and Hornebeck, W. (2009) Control of melanoma invasiveness by anticollagenolytic agents: a reappraisal of an old concept. *Anti-Cancer Agents Curr. Med. Chem. 9(5)*, 576-597.

(20) Terp, G. E., Cruciani, G. C., Christensen, I. T., and Jørgensen, F. S. (2002) Structural differences of matrix metalloproteinases with potential implications for inhibitor selectivity examined by the GRID/CPCA approach. *J. Med. Chem. 45(13),* 2675-2684.

(21) Nicolotti, O., Miscioscia, T. F., Leonetti, F., Muncipinto, G., and Carotti, A. (2007) Screening of matrix metalloproteinases available from the protein data bank: insights into biological functions, domain organization, and zinc binding groups. *J. Chem. Inf. Model. 47(6),* 2439-2448.

(22) Kontogiorgis, C. A., Papaioannou, P., and Hadjipavlou-Litina, D. J. (2005) Matrix metalloproteinase inhibitors: a review on pharmacophore mapping and (Q)SARs results. *Curr. Med. Chem. 12(3),* 339-355.

(23) Pirard, B. (2007) Insight into the structural determinants for selective inhibition of matrix metalloproteinases. *Drug Discov. Today 12(15-16),* 640-646.

(24) Cuniasse, P., Devel, L., Makaritis, A., Beau, F., Georgiadis, D., Matziari, M., Yiotakis, A., and Dive, V. (2005) Future challenges facing the development of specific active-site-directed synthetic inhibitors of MMPs. *Biochimie*, *87(3-4),* 393-402.

(25) Rao, G. B. (2005) Recent Developments in the Design of Specific Matrix Metalloproteinase Inhibitors aided by Structural and Computational Studies. *Curr. Pharm. Des. 11(3),* 295-322.

(26) Lovejoy, B., Welch, A. R., Carr, S., Luong, C., Broka, C., Hendricks, R. T., Campbell, J. A., Walker, K. A., Martin, R., Van, Wart H., et al. (1999) Crystal structures of MMP-1 and -13 reveal the structural basis for selectivity of collagenase inhibitors. *Nat. Struct. Biol. 6(3),* 217-221.

(27) Serra, P., Bruczko, M., Zapico, J. M., Puckowska, A., García, M. A., Martín-Santamaría, S., Ramos, A., and de Pascual-Teresa, B. (2012) MMP-2 Selectivity in Hydroxamate-type Inhibitors. *Curr. Med. Chem. 19(36)*, 1036-1064.

(28) Miller, A., Askew, M., Beckett, R. P., Bellamy, C. L., Bone, E. A., Coates, R. E., Davidson, A. H., Drummond, A. H., Huxley, P., Martin, F. M., et al. (1997) Inhibition of Matrix Metalloproteinases: An examination of the S1′ pocket. *Bioorg. Med. Chem. Lett. 7(2),* 193-198.

(29) Broadhurst, M. J., Brown, P. A., Johnson, W. H., and Lawton, G. (1994) European Patent Application EP-575,844-A, 1993: *Chem. Abstr. 121*, 57993.

(30) Whittaker, M., Floyd, C. D., Brown, P., and Gearing, A. J. H. (1999) Design and therapeutic application of matrix metalloproteinase inhibitors. *Chem. Rev. 99(9),* 2735-2776.

(31) Levy, D. E., Lapierre, F., Liang, W., Ye, W., Lange, C. W., Li, X., Grobelny, D., Casabonne, M., Tyrrell, D., Holme, K., et al. (1998) Matrix Metalloproteinase Inhibitors: A Structure−Activity Study. *J. Med. Chem. 41(2)*, 199-223.

(32) Zhao, Z., Raftery, M. J., Niu, X. M., Daja, M. M., and Russell, P. J. (2004) Application of in-gel protease assay in a biological sample: characterization and identification of urokinase-type plasminogen activator (uPA) in secreted proteins from a prostate cancer cell line PC-3. *Electrophoresis 25(7-8),* 1142-1148.

(33) Funovics, M., Weissleder, R., and Tung, C. H. (2003) Protease sensors for bioimaging. *Anal. Bioanal. Chem. 377(6),* 956-963.

(34) Murphy, G., Nguyen, Q., Cockett, M. I., Atkinson, S. J., Allan, J. A., Knight, C. G., Willenbrock, F., and Docherty, A. J. (1994) Assessment of the role of the fibronectin-like domain of gelatinase A by analysis of a deletion mutant. *J. Biol. Chem. 269(9),* 6632-6636.

(35) Knight, C. G., Willenbrock, F., and Murphy, G. (1992) A novel coumarin-labelled peptide for sensitive continuous assays of the matrix metalloproteinases. *FEBS Lett. 296(3),* 263-266.

(36) Pham, W., Choi, Y., Weissleder, R., and Tung, C. H. (2004) Developing a peptide-based near-infrared molecular probe for protease sensing. *Bioconjug. Chem. 15(6),* 1403-1407.

(37) McIntyre, J. O., and Matrisian, L. M. (2003) Molecular imaging of proteolytic activity in cancer. *J. Cell Biochem. 90(6),* 1087-1097.

(38) McIntyre, J. O., Fingleton, B., Wells, K. S., Piston, D. W., Lynch, C. C., Gautam, S., and Matrisian, L. M. (2004) Development of a novel fluorogenic proteolytic beacon for in vivo detection and imaging of tumour-associated matrix metalloproteinase-7 activity. *Biochem. J. 377(Pt 3),* 617-628.

(39) Bremer, C., Bredow, S., Mahmood, U., Weissleder, R., and Tung, C. H. (2001) Optical imaging of matrix metalloproteinase-2 activity in tumors: feasibility study in a mouse model. *Radiology 221(2),* 523-529.

(40) Bremer, C., Tung, C. H., and Weissleder, R. (2001) In vivo molecular target assessment of matrix metalloproteinase inhibition. *Nat. Med. 7(6),* 743-748.

(41) Zhao, M., Josephson, L., Tang, Y., and Weissleder, R. (2003) Magnetic sensors for protease assays. *Angew. Chem. Int. Ed. Engl. 42(12),* 1375-1378.

(42) Harris, T. J., von Maltzahn, G., Derfus, A. M., Ruoslahti, E., and Bhatia, S. N. (2006) Proteolytic actuation of nanoparticle self-assembly. *Angew. Chem. Int. Ed. Engl. 45(19),* 3161-3165.

(43) Lepage, M., Dow, W. C., Melchior, M., You, Y., Fingleton, B., Quarles, C. C., Pépin, C., Gore, J. C., Matrisian, L. M., and McIntyre, J. O. (2007) Noninvasive detection of matrix metalloproteinase activity in vivo using a novel magnetic resonance imaging contrast agent with a solubility switch. *Mol. Imaging 6(6),* 393-403.

(44) Medintz, I. L., Clapp, A. R., Brunel, F. M., Tiefenbrunn, T., Uyeda, H. T., Chang, E. L., Deschamps, J. R., Dawson, P. E., and Mattoussi, H. (2006) Proteolytic activity monitored by fluorescence resonance energy transfer through quantum-dot-peptide conjugates. *Nat. Mater. 5(7),* 581-589.

(45) Chang, E., Miller, J. S., Sun, J., Yu, W. W., Colvin, V. L., Drezek, R., and West, J. L. (2005) Protease-activated quantum dot probes. *Biochem. Biophys. Res. Commun. 334(4),* 1317-1321.

(46) Stockholm, D., Bartoli, M., Sillon, G., Bourg, N., Davoust, J., and Richard, I. (2005) Imaging calpain protease activity by multiphoton FRET in living mice. *J. Mol. Biol*. *346(1),* 215-222.

(47) Shi, L., De Paoli, V., Rosenzweig, N., and Rosenzweig, Z. (2006) Synthesis and application of quantum dots FRET-based protease sensors. *J. Am. Chem. Soc*. *128(32),* 10378-10379.

(48) Kim, Y. P., Oh, Y. H., Oh, E., Ko, S., Han, M. K., and Kim, H. S. (2008) Energy transfer-based multiplexed assay of proteases by using gold nanoparticle and quantum dot conjugates on a surface. *Anal. Chem*. *80(12),* 4634-4641.

(49) Kim, J. H., and Chung, B.H. (2010) Proteolytic fluorescent signal amplification on gold nanoparticles for a highly sensitive and rapid protease assay. *Small 6(1),* 126-131.

(50) Smith, R., Sewell, S. L., and Giorgio, T. D. (2008) Proximity-activated nanoparticles: in vitro performance of specific structural modification by enzymatic cleavage. *Int. J. Nanomedicine 3(1),* 95-103.

(51) Yao, H., Zhang, Y., Xiao, F., Xia, Z., and Rao, J. (2007) Quantum dot/bioluminescence resonance energy transfer based highly sensitive detection of proteases. *Angew. Chem. Int. Ed. Engl*. *46(23),* 4346-4349.

(52) Xia, Z., Xing, Y., So, M. K., Koh, A. L., Sinclair, R., and Rao, J. (2008) Multiplex detection of protease activity with quantum dot nanosensors prepared by intein-mediated specific bioconjugation. *Anal. Chem*. *80(22),* 8649-8655.

(53) Zhang, Y., So, M. K., and Rao, J. (2006) Protease-modulated cellular uptake of quantum dots. *Nano Lett. 6(9),* 1988-1992.

(54) Sewell, S. L., and Giorgio, T. D. (2009) Synthesis and enzymatic cleavage of dual-ligand quantum dots. *Mater. Sci. Eng., C 29(4),* 1428-1432.

(55) Michaluk, P., Mikasova, L., Groc, L., Frischknecht, R., Choquet, D., and Kaczmarek, L. (2009) Matrix metalloproteinase-9 controls NMDA receptor surface diffusion through integrin beta1 signaling. *J. Neurosci. 29(18),* 6007-6012.

(56) Bonoiu, A., Mahajan, S. D., Ye, L., Kumar, R., Ding, H., Yong, K. T., Roy, I., Aalinkeel, R., Nair, B., Reynolds, J. L., et al. (2009) MMP-9 gene silencing by a quantum dot-siRNA nanoplex delivery to maintain the integrity of the blood brain barrier. *Brain Res. 1282*, 142-155.

(57) Marcq, V., Mirand, C., Decarme, M., Emonard, H., and Hornebeck, W. (2003) MMPs inhibitors: New succinylhydroxamates with selective inhibition of MMP-2 over MMP-3. *Bioorg. Med. Chem. Lett. 13(17)*, 2843-2846.

(58) Moroy, G., El Mourabit, H., Toribio, A., Denhez, C., Dassonville, A., Decarme, M., Renault, J. H., Mirand, C., Bellon, G., Sapi, J., et al. (2007) Simultaneous presence of unsaturation and long alkyl chain at P1' of Ilomastat confers selectivity for gelatinase A (MMP-2) over gelatinase B (MMP-9) inhibition as shown by molecular modelling studies. *Bioorg. Med. Chem. 15(14),* 4753-4766.

(59) Phillips, R. S., and Cohen, L. A. (1986) Intramolecular general acid and general base catalyses in the hydrolysis of 2-halotryptophans and their analogs. *J. Am. Chem. Soc. 108(8)*, 2023-2030.

(60) Colletti, S. L., Li, C., Fisher, M., Wyvratt, M., and Meinke, P. (2000) Tryptophan-replacement and indole-modified apicidins: synthesis of potent and selective antiprotozoal agents. *Tetrahedron Lett. 41(41)*, 7825-7829.

(61) LeDour, G., Moroy, G., Rouffet, M., Bourguet, E., Guillaume, D., Decarme, M., ElMourabit, H., Augé, F., Alix, A. J. P., Laronze, J. Y., et al. (2008) Introduction of the 4-(4-bromophenyl)benzenesulfonyl group to hydrazide analogs of Ilomastat leads to potent gelatinase-B (MMP-9) inhibitors with improved selectivity. *Bioorg. Med. Chem. 16(18),* 8745-8759.

(62) Huey, R., Morris, G. M., Olson, A. J., and Goodsell, D. S. (2007) A semiempirical free energy force field with charge-based desolvation. *J. Comput. Chem. 28(6)*, 1145-1152.

(63) Morris, G. M., Goodsell, D. S., Halliday, R. S., Huey, R., Hart, W. E., Belew, R. K., and Olson, A. J. (1998) Automated Docking Using a Lamarckian Genetic Algorithm and an Empirical Binding Free Energy Function. *J. Comput. Chem. 19(14),* 1639-1662.

(64) Babine, R. E., and Bender, S. L. (1997) Molecular recognition of protein-ligand complexes: Applications to drug design. *Chem. Rev*. *97*, 1359-1472.

(65) Fujisawa, T., Igeta, K., Odake, S., Morita, Y., Yasuda J., and Morikawa, T. (2002) Highly water-soluble matrix metalloproteinases inhibitors and their effects in a rat adjuvant-induced arthritis model. *Bioorg. Med. Chem. 10(8)*, 2569-2581.

(66) Bourguet, E., Hornebeck, W., Sapi, J., Alix, A. J. P., and Moroy, G. (2012) Pharmacomodulation of broad spectrum matrix metalloproteinase inhibitors towards regulation of gelatinases. Enzyme Inhibition and Bioapplications. InTech Publisher.

(67) Yamamoto, M., Tsujishita, H., Hori, N., Ohishi, Y., Inoue, S., Ikeda, S., and Okada, Y. (1998) Inhibition of membrane-type 1 matrix metalloproteinase by hydroxamate inhibitors: an examination of the subsite pocket. *J. Med. Chem. 41(8)*, 1209-1217.

(68) LeDour G. (2005) Synthèse de nouveaux inhibiteurs potentiels de métalloprotéinases matricielles (MMPs), PhD Thesis, Université de Reims Champagne-Ardenne.

(69) Polette, M., Huet, E., Birembaut, P., Maquart, F. X., Hornebeck, W., and Emonard H. (1999) Influence of oleic acid on the expression, activation and activity of gelatinase A produced by oncogene-transformed human bronchial epithelial cells. *Int. J. Cancer 80(5)*, 751-755.

(70) Hermanson, G. T. (1996) Bioconjugate Techniques, Academic Press: San Diego.

(71) Green, N. M. (1990) Avidin and streptavidin. *Methods Enzymol. 184*, 51-67.

(72) Schmidt, U., and Weinbrenner, S. (1996) Preparation of 2-Bromo-5-hydroxytryptophans. *Synthesis* 28-30.

(73) Mittal, R., and Bruchez, M. P. (2011) Biotin-4-fluorescein based fluorescence quenching assay for determination of biotin binding capacity of streptavidin conjugated quantum dots. *Bioconjug. Chem*. *22(3),* 362-368.

(74) Clarke, S., Pinaud, F., Beutel, O., You, C., Piehler, J., and Dahan, M. (2010) Covalent monofunctionalization of peptide-coated quantum dots for single-molecule assays. *Nano Lett*. *10(6),* 2147-2154.

(75) La Rocca, G., Pucci-Minafra, I., Marrazzo, A., Taormina, P., and Minafra, S. (2004) Zymographic detection and clinical correlations of MMP-2 and MMP-9 in breast cancer sera. *Br. J. Cancer 90(7),* 1414-1421.

(76) Zucker, S., Lysik, R. M., Zarrabi, M. H., and Moll, U. (1993) M(r) 92,000 type IV collagenase is increased in plasma of patients with colon cancer and breast cancer. *Cancer Res. 53(1),* 140-146.

(77) Roy, R., Yang, J., and Moses, M. A. (2009) Matrix metalloproteinases as novel biomarkers and potential therapeutic targets in human cancer. *J. Clin. Oncol*. *27(31),* 5287-5297.

(78) Akinfieva, O., Nabiev, I., and Sukhanova, A. (2012) New directions in quantum dot-based cytometry detection of cancer serum markers and tumor cells. *Crit. Rev. Oncol. Hematol*. 86, 1-14.

(79) Morgunova, E., Tuuttila, A., Bergmann, U., Isupov, M., Lindqvist, Y., Schneider, G., and Tryggvason, K. (1999) Structure of human pro-matrix metalloproteinase-2: activation mechanism revealed. *Science 284(5420)*, 1667-1670.

(80) Rowsell, S., Hawtin, P., Minshull, C. A., Jepson, H., Brockbank, S. M., Barratt, D. G., Slater, A. M., McPheat, W. L., Waterson, D., Henney, A. M., et al. (2002) Crystal structure of human MMP9 in complex with a reverse hydroxamate inhibitor. *J. Mol. Biol.* 3*19(1)*, 173-181.

(81) Li, H., Robertson, A. D., and Jensen, J. H. (2005) Very fast empirical prediction and rationalization of protein pKa values. *Proteins 61(4),* 704-721.

(82) Bas, D. C., Rogers, D. M., and Jensen, J. H. (2008) Very fast prediction and rationalization of pKa values for protein-ligand complexes. *Proteins 73(3),* 765-783.

(83) Mehler, E. L., and Solmajer, T. (1991) Electrostatic effects in proteins: comparison of dielectric and charge models. *Protein Eng. 4(8)*, 903-910.

Graphical abstract